

**BEARING CAPACITY OF ECCENTRICALLY LOADED  
EMBEDDED SQUARE FOOTING  
ON GEOGRID REINFORCED SAND**

**A THESIS SUBMITTED  
IN PARTIAL FULFILLMENT OF THE REQUIREMENT  
FOR THE AWARD OF THE DEGREE  
OF  
MASTER OF TECHNOLOGY  
IN  
CIVIL ENGINEERING**



**ANNAPURNA MAHANTA**

**DEPARTMENT OF CIVIL ENGINEERING**

**NATIONAL INSTITUTE OF TECHNOLOGY, ROURKELA**

**ODISHA-769008**

**MAY-2015**

**BEARING CAPACITY OF ECCENTRICALLY LOADED EMBEDDED  
SQUARE FOOTING ON GEOGRID REINFORCED SAND**

*In partial fulfillment of the requirements for the award of the degree of*

**MASTER OF TECHNOLOGY  
IN  
CIVIL ENGINEERING**

*Guided by*

**DR C R PATRA**

*Submitted By*

**ANNAPURNA MAHANTA**

**ROLL NO-213CE1046**



**DEPARTMENT OF CIVIL ENGINEERING**

**NATIONAL INSTITUTE OF TECHNOLOGY**

**ROURKELA - 769008**



## CERTIFICATE

This is to certify that the thesis entitled as “*Bearing capacity of eccentrically loaded embedded square footing resting on geogrid reinforced sand bed*” is a record of bonafide work and sincere efforts put forward by Annapurna Mahanta submitted in the partial fulfillment for the requirement of the degree of **Master of Technology in Civil Engineering** with specialization in **Geotechnical engineering** at National Institute of Technology Rourkela, under my guidance and supervision.

According to the best of my knowledge, the content in this report has not been submitted to any other university/institute for the award of any degree or diploma.

Dr Chittaranjan Patra  
Department of Civil Engineering  
National Institute of Technology  
Rourkela

## ACKNOWLEDGEMENT

I would like to express my deep sense of gratitude to my esteemed supervisor **Prof. Chittaranjan Patra**, for his encouragement and consistent support throughout the research work in the last one year. I would genuinely acknowledge his faith in me, to do this work, taking it to a higher level.

I would also like to extend my sincere thanks to **Prof. S.K. Sahu, HOD, Civil Engineering Department**, National Institute of Technology, Rourkela, who have illuminated me throughout my research work with his enormous support.

I am also honoured, for **Prof. N. Roy , Prof. S.K. Das, Prof. S.P. Singh, Prof. R.K. Bag, Prof. S. Patra, Prof. R.N. Behera** and all other faculty members of Civil Engineering Department, NIT Rourkela, having their valuable support during my research work.

Exceptional and sincere thanks to **Miss. Roma Sahu**, and **Mr. Barada Prasad Sethy** Ph.D. Scholars in Civil Engineering Department, NIT Rourkela for their valuable suggestions, remarks, emotional and consistent support during the crucial period of research work.

I am also appreciative to Mr. A. K Nanda, Technical Assistant, Geotechnical Engineering Laboratory, NIT Rourkela for his remarkable support during my research work.

At long last, I would thank my family members for their unconditional moral support, a special thanks to my mother, for being there for me, sailing my boat through all hardships.

Annapurna Mahanta

## ABSTRACT

Although lot many research works have been conducted on shallow foundations, still eccentric loadings under geogrid reinforced sand bed for different overburden depths are manifested very less. In this thesis, a sharp look has been given to the behavior of square footings under different loading conditions.

Here, a number of tests have been carried out on square footing ,of dimension, 10cm x 10cm, on reinforced sand bed. The eccentricities of the footing are varied from  $0.05B$  to  $0.15B$ , with an increment of  $0.05B$ . The biaxial geogrid used here is TGB-40, placed in varying number of layers as 0, 2, 3, 4. The embedment depth is also varied as  $0.5B$  to  $1.0B$  (where  $B$  is the width of the footing). The distance between the consecutive geogrids is maintained in a constant manner for all the experiments. A relative density of 69% is achieved during all the tests. The Settlement occurred at increasing loading rate is plotted on graphs, from where the load carrying capacity is found out using tangent intersection method. From the limited experiments conducted in the laboratory, an empirical equation has been developed to determine the load carrying capacity of square embedded footing under eccentric load resting over geogrid-reinforced sand by knowing the bearing capacity of the same footing under similar conditions but under centric load. This is achieved by use of reduction factor.

Keywords – load carrying capacity, eccentricity, embedment depth, settlement, number of geogrid layers

# CONTENTS

CHAPTER 1	INTRODUCTION	1
1.1	General	1
1.2	Objective of present study	2
CHAPTER 2	LITERATURE REVIEW	3
2.1	Bearing capacity of centric loaded	3
2.2	Bearing capacity of eccentric loading	6
2.3	Footing resting on reinforced soil bed	7
CHAPTER 3	EQUIPMENTS AND MATERIALS	13
3.1	General	13
3.2	Sand	13
3.2.1	geogrid	15
3.3	Test Tank	16
3.4	Equipment Used	17
3.4.1	Static Loading Unit	17
3.4.2	Model footing	17
3.4.3	Proving Ring	17
3.4.4	Dial Gauge	17
CHAPTER 4	MODEL TEST AND METHODOLOGY	18
4.1	Sample Preparation	18
4.2	Placement of Geogrid	18
4.3	Test procedure	20
4.4	Model test series	21
CHAPTER 5	RESULTS AND DISCUSSION	22
5.1	General	22
5.2	Model tests	22
5.2.1	Bearing capacity of unreinforced sand	23
5.2.2	Bearing capacity of reinforced sand	25
5.3	Analysis of results	37
5.3.1	Analysis of square footing with $D_f/B=0.5$	37
5.3.2	Analysis of square footing with $D_f/B=1.0$	40
CHAPTER 6	CONCLUSION	45
	REFERENCES	

## LIST OF TABLES

Table 2.1	List of bearing capacity factors	4
Table 2.2	a & K values as suggested by Purkayastha and Char	6
Table 3.1	Geotechnical Properties of Sand	14
Table 3.2	Properties of geogrid	16
Table 4	Model test series	21
Table 5.1	Comparison of load carrying capacity values with the experimental ones	24
Table 5.2	Experimental reduction factor for eccentrically loaded footing resting on reinforced sand bed with $D_f/B=0.5$	38
Table 5.3	Experimental reduction factor for eccentrically loaded footing resting on reinforced sand bed with $D_f/B=1.0$	41

## LIST OF FIGURES

Fig 3.1 Particle size distribution curve	14
Fig 3.2 Biaxial geogrid	15
Fig 3.4 Mechanism of geogrid	15
Fig 4.1 placement of geogrid layers	19
Fig 4.2 placement of geogrid in the tank	19
Fig 4.3 Equipment set up	21
Fig 5.1 Load vs settlement curve for $D_f/B=0.5$ & $N=0$ and different $e/B$ ratios	23
Fig 5.2 Load vs settlement curve for $D_f/B=1.0$ & $N=0$ and different $e/B$ ratios	23
Fig 5.3 Calculation of bearing capacity by tangent intersection method	24
Fig 5.4 Load vs settlement curve for $D_f/B=0.5$ & $N=2$ and different $e/B$ ratios	25
Fig 5.5 Load vs settlement curve for $D_f/B=0.5$ & $N=3$ and different $e/B$ ratios	26
Fig 5.6 Load vs settlement curve for $D_f/B=0.5$ & $N=4$ and different $e/B$ ratios	26
Fig 5.7 Load vs settlement curve for $D_f/B=1.0$ & $N=2$ and different $e/B$ ratios	27
Fig 5.8 Load vs settlement curve for $D_f/B=1.0$ & $N=3$ and different $e/B$ ratios	27
Fig 5.9 Load vs settlement curve for $D_f/B=1.0$ & $N=4$ and different $e/B$ ratios	28
Fig 5.10 Load vs settlement curve for $D_f/B=0.5$ & $e/B=0$ for different $N$ layers	28
Fig 5.11 Load vs settlement curve for $D_f/B=0.5$ & $e/B=0.05$ for different $N$ layers	29
Fig 5.12 Load vs settlement curve for $D_f/B=0.5$ & $e/B=0.10$ for different $N$ layers	29
Fig 5.13 Load vs settlement curve for $D_f/B=0.5$ & $e/B=0.15$ for different $N$ layers	30
Fig 5.11 Load vs settlement curve for $D_f/B=1.0$ & $e/B=0$ for different $N$ layers	30



Fig 5.15 Load vs settlement curve for $D_f/B=1.0$ & $e/B=0.05$ for different N layers	31
Fig 5.16 Load vs settlement curve for $D_f/B=1.0$ & $e/B=0.10$ for different N layers	31
Fig 5.17 Load vs settlement curve for $D_f/B=1.0$ & $e/B=0.15$ for different N layers	32
Fig 5.18 Load vs settlement curve for $N=2$ & $e/B=0$ for different $D_f/B$ depth	32
Fig 5.19 Load vs settlement curve for $N=2$ & $e/B=0.05$ for different $D_f/B$ depth	33
Fig 5.20 Load vs settlement curve for $N=2$ & $e/B=0.10$ for different $D_f/B$ depth	33
Fig 5.21 Load vs settlement curve for $N=2$ & $e/B=0.15$ for different $D_f/B$ depth	34
Fig 5.22 Load vs settlement curve for $N=3$ & $e/B=0$ for different $D_f/B$ depth	34
Fig 5.23 Load vs settlement curve for $N=3$ & $e/B=0.05$ for different $D_f/B$ depth	35
Fig 5.24 Load vs settlement curve for $N=3$ & $e/B=0.10$ for different $D_f/B$ depth	35
Fig 5.25 Load vs settlement curve for $N=3$ & $e/B=0.15$ for different $D_f/B$ depth	36
Fig 5.26 Variation of $R_{KR}$ with $d_f/B$ for $D_f/B=0.5$	39
Fig 5.27 Variation of $R_{KR}$ with $e/B$ for $D_f/B=0.5$	39
Fig 5.28 Variation of $R_{KR}$ with $e/B$ for $D_f/B=0.5$	40
Fig 5.29 Variation of $R_{KR}$ with $d_f/B$ for $D_f/B=1.0$	42
Fig 5.30 Variation of $R_{KR}$ with $e/B$ for $D_f/B=1.0$	43
Fig 5.31 Variation of $R_{KR}$ with $e/B$ for $D_f/B=1.0$	44

# Chapter 1

## INTRODUCTION

### 1.1 GENERAL

The foundation is a substructure which transfers the load to the underlying soil, placed below the superstructure. Footings are often subjected to moments from columns in addition to the axial loads. The presence of any amount of eccentricity of loading above the foundation caused for moment on the foundation. During the design of a foundation, eccentricity has to be considered carefully because increase in eccentricity beyond a certain limit would lead to a considerable decrease in area of footing which is ineffective to resist the stresses. The development of tension in the footing causes the move away of the footing from the soil. The two important parameters for the design of a foundation are the bearing capacity and the settlement of foundation. Both the criterias has to be considered carefully for the safety of a structure. The granular material is strengthened by providing the geosynthetic material due to its tensile characteristics. The significant effect of geosynthetics was developed in 19th century by Henry Vidal. Providing the geogrid in the foundation or pavement generally have 3 benefits, (i) reduces the cost of construction material (ii) serviceability of the developed model is greater as compared to the unreinforced section (iii) the shear stress reduces as we provide the geogrid reinforcement due to increase in the internal angle of fiction. As we know the soil is weak in tension, to provide the tensile properties to granular soil, we make access to geogrid materials. Due to its large aperture size, the geogrid material can interlock effectively with the granular material to form a composite material. Keeping these points in view, the

bearing capacity is determined for a embedded square footing subjected to eccentric vertical load, by providing bi-axial geogrid, in this present study.

## **1.2 OBJECTIVE OF PRESENT STUDY**

- To determine the bearing capacity of eccentrically loaded shallow square footings resting over reinforced granular material.
- If the bearing capacity of centrally loaded square footings on reinforced sand bed is known, then the bearing capacity of eccentrically loaded footing can be determined.

In the present study, a series of experiments have been conducted with

- model square footings
- placed at different depths of embedment
- Geogrid have been used as the reinforcing material in sand
- Square footings are used
- Loads are applied with different eccentricity.

## Chapter 2

### LITERATURE REVIEW

#### 2.1 Bearing capacity of centric loaded footing over unreinforced sand

**Terzaghi (1943)** proposed the bearing capacity of a strip foundation subjected to a vertical centrally applied load over a homogenous soil.

$$q_u = cN_c + qN_q + 0.5 \gamma BN_\gamma \quad \text{For continuous and strip foundation}$$

$$q_u = 1.3cN_c + qN_q + 0.4\gamma BN_\gamma \quad \text{For square foundation}$$

$$q_u = 1.3cN_c + qN_q + 0.3\gamma BN_\gamma \quad \text{For circular foundation}$$

Where,  $c$  = cohesion of soil,  $\gamma$  = unit weight of soil and  $q = \gamma D_f$

Where,  $N_c$ ,  $N_q$ ,  $N_\gamma$  are the bearing capacity factor and are given by

$$N_c = \cot\phi \left[ \frac{e^{2\left(\frac{3\pi}{4} - \frac{\phi}{2}\right)\tan\phi}}{2\cos^2\left(\frac{\pi}{4} + \frac{\phi}{2}\right)} - 1 \right]$$

$$N_q = \left[ \frac{e^{2\left(\frac{3\pi}{4} - \frac{\phi}{2}\right)\tan\phi}}{2\cos^2\left(\frac{\pi}{4} + \frac{\phi}{2}\right)} - 1 \right]$$

$$N_\gamma = \frac{1}{2} \left( \frac{K_{p\gamma}}{\cos^2\phi} - 1 \right) \tan\phi$$

where  $K_{p\gamma}$  = passive pressure coefficient

**Meyerhof (1963)** proposed a generalized equation for load carrying capacity of any shape of (whether it may be strip, rectangular or square), the equation for load carrying capacity is as follows.

$$q_u = cN_cF_{cs}F_{cd}F_{ci} + qN_qF_{qs}F_{qd}F_{qi} + \frac{1}{2}\gamma BN_\gamma F_{\gamma s}F_{\gamma d}F_{\gamma i}$$

where,  $F_{cs}$ ,  $F_{qs}$ ,  $F_{\gamma s}$  = shape factor,

$F_{cd}, F_{qd}, F_{\gamma d}$  = depth factor and

$F_{cs}, F_{qs}, F_{\gamma s}$  = inclination factor

**Vesic (1973)** considered the effect of the shape of footing and the shearing resistance of soil above the bottom of footing.

Table 2.1 List of bearing capacity factors

Bearing capacity factors	Equation	Investigator
$N_c$	$N_c = (N_q - 1) \cot \phi$	Terzaghi (1943), Meyerhof (1963)
$N_q$	$N_q = \left[ \frac{e^{2 \left( \frac{3\pi}{4} - \frac{\phi'}{2} \right) \tan \phi'}}{2 \cos^2 \left( 45 + \frac{\phi'}{2} \right)} \right]$	Terzaghi (1943)
$N_q$	$N_q = \tan^2 \left( 45 + \frac{\phi}{2} \right) e^{(\pi \tan \phi)}$	Meyerhof(1963), Hansen(1970), Vesic (1973), IS CODE(IS: 6403-1981)
$N_\gamma$	$N_\gamma = 1.8(N_q - 1) \cot \phi (\tan \phi)^2$	Terzaghi(1943)
$N_\gamma$	$N_\gamma = 1.5(N_q - 1) \tan \phi$	Hansen(1970)
$N_\gamma$	$N_\gamma = 2(N_q + 1) \tan \phi$	Vesic (1973) IS CODE (IS: 6403-1981)

Bearing capacity factors	Equation	Investigator
Shape	<p>For <math>\phi = 10^\circ</math> <math>\lambda_{cs} = 1 + 0.2 \frac{B}{L}</math></p> <p><math>\lambda_{qs} = \lambda_{\gamma s} = 1</math></p> <p>For <math>\phi \geq 10^\circ</math></p> <p><math>\lambda_{cs} = 1 + 0.2 \frac{B}{L} \tan^2 \left( 45 + \frac{\phi}{2} \right)</math></p> <p><math>\lambda_{qs} = \lambda_{\gamma s} = 1 + 0.1 \frac{B}{L} \tan^2 \left( 45 + \frac{\phi}{2} \right)</math></p>	Meyerhof (1963)
	<p><math>S_q = 1 + \left( \frac{B}{L} \right) \tan \phi</math></p> <p><math>S_\gamma = 1 - 0.4 \left( \frac{B}{L} \right)</math></p>	<p>Vesic (1975)</p> <p>Hansen(1970)</p>
Depth	<p><math>\phi \geq 10^\circ : d_c = 1 + 0.2 \left( \frac{D_f}{B} \right) \tan \left( 45 + \frac{\phi}{2} \right)</math></p> <p><math>d_q = d_\gamma = 1 + 0.1 \left( \frac{D_f}{B} \right) \tan \left( 45 + \frac{\phi}{2} \right)</math></p>	Meyerhof(1963)
	<p>For <math>\frac{D_f}{B} \leq 1 : d_c = d_q - \frac{1 - d_q}{N_q \tan \phi} (For \phi &gt; 0)</math></p> <p><math>d_q = 1 + 2 \tan \phi (1 - \sin \phi)^2 \left( \frac{D_f}{B} \right)</math></p> <p><math>d_\gamma = 1</math></p>	<p>Hansen(1970)</p> <p>Vesic(1975)</p>
	$d_q = d_\gamma = 1 + 0.1 \left( \frac{D_f}{B} \right) \sqrt{\tan^2 \left( 45 + \frac{\phi}{2} \right)} (For \phi > 10^\circ)$	IS CODE (IS: 6403-1981)

## 2.2 Bearing capacity of eccentric loading

**Prakash and Saran (1971)** proposed a relationship to evaluate the ultimate load per unit length of strip foundation subjected to vertical eccentric load according to the following equation

$$q_{ult} = B \left[ cN_{c(e)} + qN_{q(e)} + \frac{1}{2} \gamma B N_{\gamma(e)} \right]$$

Where,  $N_{c(e)}$ ,  $N_{q(e)}$  and  $N_{\gamma(e)}$  are the bearing capacity factors for the case of eccentric loading.

**Purkayastha and Char (1977)** used method of slices to investigate the eccentrically loaded strip footing resting on sand layer. Based on their study, they proposed a correlation of reduction factor which is given as

$R_k$  = reduction factor

$$R_k = a \left( \frac{e}{B} \right)^k$$

Table 2.2  $a$  &  $K$  values as suggested by Purkayastha and Char

$D_f/B$	$a$	$K$
0.00	1.862	0.73
0.25	1.811	0.785
0.50	1.754	0.80
1.00	1.820	0.888

Now the load carrying capacity of eccentrically loaded strip footing is given by

$$q_{u(eccentric)} = q_{u(centric)} (1 - R_k)$$

$$q_{u(centric)} = qN_q F_{qd} + \frac{1}{2} B \gamma F_{\gamma d}$$

**Highters and Anders (1985)** proposed different type of equations to find out the effective area of rectangular footing by considering eccentricity in both direction. Different cases of eccentricity were considered according to different  $e/B$  and  $e/L$  ratios.

### **2.3 Footing resting on reinforced soil bed**

**Huang and Tatsuoka(1990)** conducted a series of plain strain model tests on strip footing upon reinforced sand bed. The number of layers, the length of each reinforcement and the horizontal distance between, and the stiffness and rupture strength of reinforcement, were checked out. According to the results, as observed from the experiments, a limit equilibrium method was found out, for stability analysis, by considering the arrangement and the properties of reinforcement and the failure mode of reinforced sand, beneath the footing. A length similar to the footing width of reinforcement layer, would considerably increase the bearing capacity to a great extent.

**Khing *et al.* (1993)** performed a number of laboratory-model tests of strip footing reinforced with geogrid layers. The maximum bearing capacity is achieved when the depth of the first reinforcing layer was less than the footing width. If the geogrid is placed, at a depth more than, 2.25 times the width of the footing, would hardly affect the bearing capacity. The minimum width of the geogrid layers should be around six times the footing width. The bearing-capacity ratio calculated on the basis of limited settlement appears to be about 67-70% of the ultimate bearing-capacity ratio.

**Omar *et al.* (1993)** investigated the effect of width to length ratio ( $B/L$ ) of footings on the BCR with geogrid reinforcement. The results showed that the influence depth of reinforcement is inversely proportional to the width to length ratio ( $B/L$ ) of the footing. It was about  $2B$  for strip footing and  $1.2B$  for square footing. The influence depth is the total



reinforcement depth below which, if we place also reinforcement layer, the effect in the BCR is not noticeable. The maximum BCR also decreased with the increase of the  $B/L$  of the footing for  $u/B$  and  $h/B$  ratios of 0.33 and 0.33 with optimum reinforcement arrangement.

**Yetimoglu *et al.* (1994)** carried out a number of laboratory tests and also finite element analyses, to investigate the bearing capacity of geogrid reinforced sand bed. They proposed that, for the multilayered reinforced sands greatest BCR values occurred at a depth ratio (ratio of settlement to the width of the footing) of around 0.25, and BCR became much smaller when the depth ratio was greater than about 0.9. The BCR increased proportionally with the number of reinforcement layers up to  $N=4$ . For multilayer reinforced sand, the highest bearing capacity occurs when the depth of embedment approximately is  $0.25B$ . The optimum spacing for the reinforced sand between two layers is between  $0.2B$  and  $0.4B$ . From the conducted experiments, it showed that the effective zone is within  $1.5B$  from the ends and the base of the footing.

**Das and Omar (1994)** studied the effects of footing width on BCR of model tests on geogrid reinforced sand. A number of laboratory tests on bearing capacity of unreinforced and geogrid-reinforced sand were conducted using model strip foundations of different width. Different width of the footing and different relative density was maintained for the sand to study their effects on the bearing capacity ratio. The bearing capacity ratio of it decreases with an increase in the width of the foundation and practically reaches a constant value when the width is equal to or greater than 130-140mm.

**Huang and Menq(1997)** performed as many as 105 experiments to find out the characteristics of bearing capacity of sand, when, it is reinforced with horizontal layers. Here a quasi-rigid, earth slab is formed below the base of the footing, which effects the bearing

capacity, when reinforcements were induced in it. Generally two failure mechanisms, i.e. deep-footing and wide-slab mechanism characterizes the bearing capacity characteristics. Based on the experimental work and the analysis of, the load carrying capacity equation ,for wide-slab mechanism was proposed as,

$$q_u = 0.5(B + \Delta B)\gamma N_\gamma + D_f N_q$$

where,

$$\Delta B = d \tan \beta$$

$\gamma$  = working density of sand

$B$  = width of the footing

$N_\gamma, N_q$  = bearing capacity factors

$d$  = depth of the placement of the last reinforcement from the base of the footing

$$d = u + (N - 1)h$$

here,  $u$  = depth of the first layer of reinforcement from the base of footing,

$N$  = no of geogrid layers

and ,  $h$  = distance between two consecutive geogrid layers

$\beta$  = spreading angle

where,  $\beta$  is given by

$$\tan \beta = 0.68 - 2.071 \left( \frac{h}{B} \right) + 0.743(CR) + 0.03 \left( \frac{b}{B} \right)$$

where,  $CR$  = cover ratio, i.e. width of longitudinal ribs to c/c spacing of

longitudinal ribs ( $w/W$ )

**Shin *et al.* (2002)** conducted a number of laboratory model tests on granular soil with multiple geogrid layers to determine the load carrying capacity of a strip foundation working on the influence of embedment. The critical reinforcement-depth ratio below the bottom of the

foundation  $(d/B)_{cr}$  for deriving the maximum benefit from reinforcement is about 2. The relationship between the bearing capacity ratio at ultimate load and at limited levels of settlement (less than or equal to 5% of foundation width) was also presented. The bearing capacity ratio at limited levels of settlement is smaller than the value at ultimate load.

**Sitharam *et al.* (2005)** conducted a number of experiments on embedded circular footing supported on geogrid cell reinforced foundation bed. The variation of embedment depth of the footing was from 0 to 0.6 times the footing width over foundation beds made of dry sand and saturated silty clay. The bearing pressure-Settlement response of the embedded circular footing supported on cellular reinforced beds is almost linear up to a settlement range of 12–15% of the footing width in sand bed and about 8–10 % in clay bed. The load carrying capacity of the reinforced sand beds increased by 9.5 times with increase in the embedment depth of foundation and about 6.5 times in the surface case. In case of reinforced soft clay beds, bearing capacity increased against the unreinforced bed, and it increased up to 5.5 with the footing embedment depth. In sand, it could be said that at allowable settlement range of isolated footings, the footing embedment depth equal to  $0.3D$  gives optimal performance.

**Patra *et al.* (2006)** conducted a number of model tests to determine the load carrying capacity of geogrid-reinforced sand subjected to eccentric loads. Based on the laboratory test results, an empirical relationship called reduction factor,  $R_k$  was found out which, correlates the ratio of the load carrying capacity of a foundation subjected to eccentric load, with that of centrally loaded one.

$$R_k = 4.97 \left( \frac{d_f}{B} \right)^{-0.21} \left( \frac{e}{B} \right)^{1.21}$$

**Omar (2006)** conducted a number of model tests to determine the load carrying capacity of geogrid-reinforced sand subjected to eccentric loads. Based on the laboratory model test, an

empirical relationship for reduction factor has been developed. If the bearing capacity of centric loaded footing is known, then this reduction factor can be used to, find out the bearing capacity, that of an eccentrical one.

$$R_k = 5.11 \left( \frac{D_f}{B} \right)^{-0.14} \left( \frac{e}{B} \right)^{1.21}$$

**Latha and Somwanshi (2009)** conducted a number of laboratory model test and performed numerical simulation result for bearing capacity of geosynthetic reinforced sand subjected to square footing. The effect of different reinforcement parameters such as the type and tensile strength of geosynthetic materials, number of reinforcement layers, arrangement and the configuration of geosynthetic layers below the footing was taken into account. The experimental result showed that the effective depth of the zone of reinforcement below footing was  $2B$ , and the optimum spacing of consecutive reinforcement layers was about 0.4 times the width of footing and the optimum width of reinforcement is  $4B$ , where  $B$  is the width of the footing.

**Sadoglu *et al.* (2009)** conducted a number of laboratory model tests on geotextile-reinforced dense sand with strip footing subjected to eccentric loading and to investigate how the eccentricity affect the load carrying capacity of foundation. Experimental results found from it were compared with the Meyerhof's (1953) effective width concept.

**Tirkity and Taay(2012)** they investigated the geogrid reinforcement effect on the eccentrically loaded bearing capacity of strip footing PLAXIS 2D was used for numerical analysis using finite element program. The results showed that increasing the number of geogrid layers ( $N$ ) significantly increased the load carrying capacity, but there was an optimum value after which little effect was observed. These optimum value were varied ( $N=3-4$ ) depending on the value of load eccentricity ratio ( $e/B$ ) and depth of footing ( $D_f/B$ ).

Increasing the depth of footing ( $D_f/B$ ) does not affect the optimum value of ( $N$ ), but it does significantly increase the load carrying capacity and unlike the effect of ( $N$ ) it has a significant effect on the reduction that is due to the eccentricity ratio ( $e/B$ ). Increasing the angle of internal friction ( $\phi$ ) increased the load carrying capacity. But it had no effect on the optimum value of ( $N$ ) or the optimum values of ( $u/B$ ) and ( $h/B$ ).

**Nareeman (2012)** performed experiments on circular, square and rectangular footing to study the effect of scale on bearing capacity and settlement of footing. The experimental results were compared with that of FEA. Experimental results showed that the bearing capacity factor  $N_\gamma$  depends on the absolute width of the footing and it decreases with that in increase of footing and  $S_\gamma$  increased with that of footing width.

**Kolay *et al.* (2013)** determined the load carrying capacity of silty clayey soil with geogrid reinforcement. In this study a thin layer of sand was provided on the top of the silty clay soil. They suggested that by providing layers of geogrid reinforcement, the bearing capacity changes, according to different  $u/B$  and  $h/B$  ratios.

### MATERIALS AND EQUIPMENTS

#### 3.1 General

The experimental set up designed in this study, aim at investigating the potential benefits of using the reinforced soil foundations using geogrid to improve the bearing capacity and to reduce the settlement of shallow foundations in soil. Here, fine to medium sand is used as the geomaterial, and, techgrid biaxial geogrid is used as the reinforcement material. The model tests are carried out on square footings, with varying eccentricities from  $0.05B$  to  $0.15B$  (where  $B$  is the width of the footing).

#### 3.2 MATERIALS USED

##### 3.2.1 Sand

##### 3.2.2 SAMPLE COLLECTION

The sand which we use in our experiment is collected from the nearby flowing Koel river. It underwent through cleaning process, by washing the sand and removing the debris from it, like, the leaves, organic particles, twigs, etc. Then it was oven dried, and was made to pass through sieve through various sizes, it was supposed to pass through  $710\mu$  sieve and retained through  $300\mu$  sieve size. And the retaines sample was used in our experimental work.

##### 3.2.3 CHARACTERISTICS OF SAND

The experiments are conducted in medium dense sand, achieving relative density as 69%. The particle size distribution curve of the sand sample is shown in fig 3.1. The coefficient of angle of friction is found out to be  $40.8^\circ$  for the desired density of the sample by direct shear test. The geotechnical properties of sand are enlisted in the table below.

Table 3.1: Geotechnical Properties of Sand

PROPERTY	MAGNITUDE
Specific gravity, $G$	2.63
Uniformity coefficient, $C_u$	1.30
Coefficient of curvature, $C_c$	1.11
Relative density, $I_d$	69%
Maximum unit weight, $\gamma_{max}$	15.08kN/m <sup>3</sup>
Minimum unit weight, $\gamma_{min}$	12.9kN/m <sup>3</sup>
Working density, $\gamma_d$	14.32 kN/m <sup>3</sup>
Internal angle of friction, $\phi$	40.8°

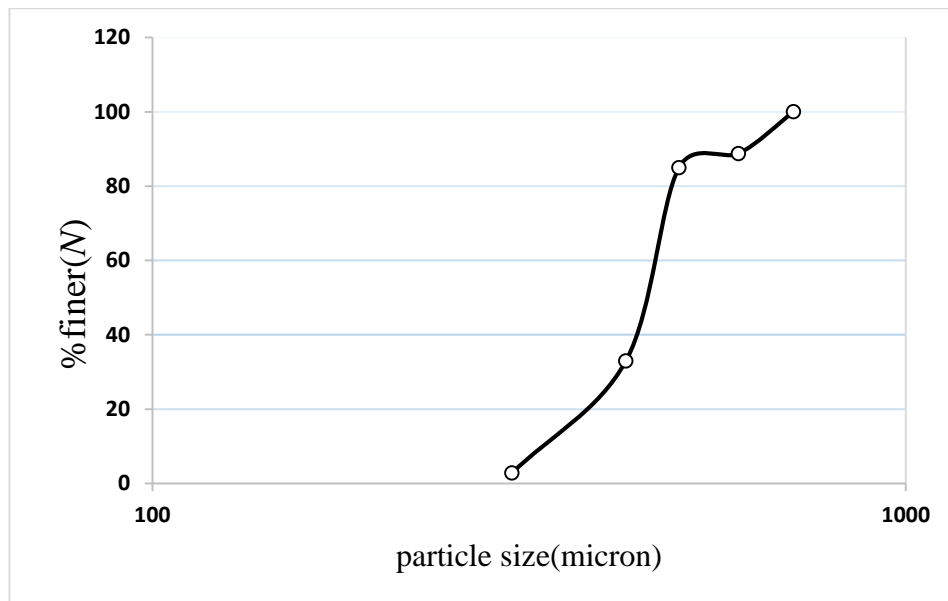


Fig 3.1 particle size distribution curve

From the grain size distribution curve, we infer that , the soil medium, or the sand which we use in our experiment is uniformly graded or poor graded.

### 3.2.2 GEOGRID

Geogrids are planar, polymeric structures consisting of a regular open network of integrally connected tensile elements, which may be linked by bonding or interlacing, openings of which are larger than the constituents. In civil engineering applications geogrids are used in contact with soil or rock and/or any other geotechnical material. These openings are called as apertures, which allow sand particle to come in to direct contact on either side of the mounted geogrid which increases the interaction between the geogrid and sand increasing the tensile strength of sand fill. Features of the geogrid varies in polymer type and cross-sectional proportions. When the soil strains in response to applied loads, tensile forces are generated in the geogrid because of the frictional interaction between the geogrid and the soil. The tensile forces developed in the reinforcement keeps the reinforced soil mass in stable equilibrium. The mechanism of Bi-axial geogrid is shown in figure below.



Fig 3.2 Biaxial geogrid

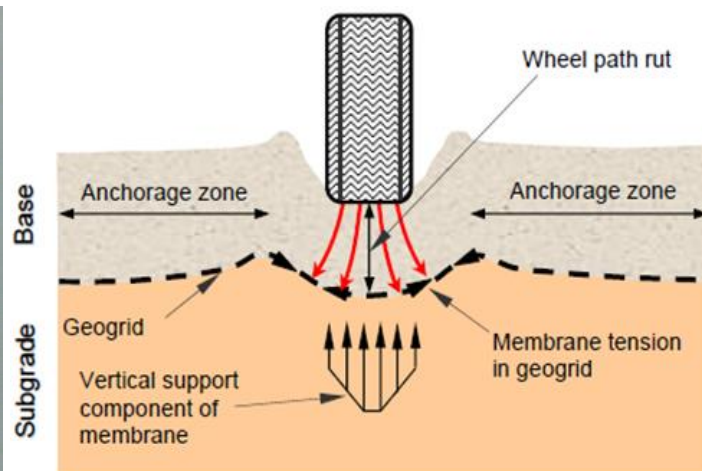


Fig 3.3 Mechanism of geogrid



Table 3.2 properties of geogrid

Polymer	Ultimate tensile strength (kN/m)		Elongation at maximum load (%)		Tensile strength at 2% elongation (kN/m)		Tensile strength at 5% elongation (kN/m)	
	MD	CD	MD	CD	MD	CD	MD	CD
<b>Polyster</b>	40	40	15	15	7.5	7.5	14	14

### 3.3 TEST TANK

The tank which we use here has the dimension of 100cm length x 50.4cm width x 65cm width. The dimensions are adopted after doing various literature studies. As per IS 1888-1962, the width of the test pit should be at least five times the width of the footing, so that the failure zones can develop freely, without any interference effect. For cohesionless soil, Chumar (1972) suggested that the maximum extension of failure zone would be 2.5 times of the footing width along the side and three times footing width below it. The length sides were made from 12mm thick fibre glass, and the width sides are made from mild steel of thickness 8mm. Scales are mounted at different intervals, to maintain different height of fall, to achieve the desired density. All the four sides are braced to avoid bulging due to sand fill. Scales are provided at various positions to maintain the height of fall, while achieving the desired density.

### 3.4 EQUIPMENTS USED

#### 3.4.1 LOAD TRANSFERRING SHAFT

A manually operated static loading unit is used to apply the load on the foundation during test. The whole loading unit consist of rotating axle and one loading frame with shaft. The axle is rotated manually with a uniform speed to control the movement of shaft.

#### 3.4.2 MODEL FOOTING

Model footing are of mild steel of dimension 10cm x 10cm, having thickness of 3cm. Four different footings are used, according to varied conditions ,one is for centric loading, and three other for eccentric loading, eccentricity varying from,  $0.05B$  to  $0.15B$ , and circular grooves are drilled into it, to fit the ball, which is in connection to the shaft, to take the load according to different eccentric or centric conditions. The other face of the footing is made rough, by adhering sand with epoxy glue, to make the surface rough, so that, proper friction develops, during the application of load.

#### 3.4.3 PROVING RING

Proving rings of (10kN, 12kN & 20kN) are used to measure the applied load during the experiment according to different loading conditions, to accurately measure the loading increment.

#### 3.4.4 DIAL GAUGE

Two dial gauges of least count 0.01mm are used, to measure the settlement, from the applied loads. These are placed at opposite corners of the footing diagonally, to measure the average settlement of the footing on the opposite sides. The dial gauge is supported by magnetic base, which in turn clinches on the test tank.

## Chapter 4

### MODEL TEST AND METHODOLOGY

#### 4.1 SAMPLE PREPARATION

At first the internal dimensions of the tank are measured accurately and volume for the required fill is calculated, taking the working density to be 1.46g/cc. Now, by adopting rain falling technique, the box is filled with sand, and by maintaining different height of fall achieve the desired relative density of the sand for the experiments to be conducted. After several trials, as the relative density is achieved by maintaining different height of fall, it is spread in 2.5cm layers through rain falling technique, which takes around 18.45kg for each layer, which is found out from the calculation. After each fall, the sand layer is levelled by means of a scale.

#### 4.2 PLACEMENT OF GEOGRIDS

In this present study the geogrid has been placed as  $(u/B) = 0.35$ ,  $(b/B) = 4.5$  &  $(h/B) = 0.25$ .

Since it is a reinforced soil sample, geogrids are placed horizontally in between at desired depth from bottom of footing after levelling the surface. After literature surveys, it has been found that for strip footing and square footing  $(u/B)_{cr}$  vary between 0.25 and 0.5 and  $(b/B)_{cr}$  is 8 and 4.5 respectively and  $(h/B)_{cr}$  lies between 0.25 to 0.4.

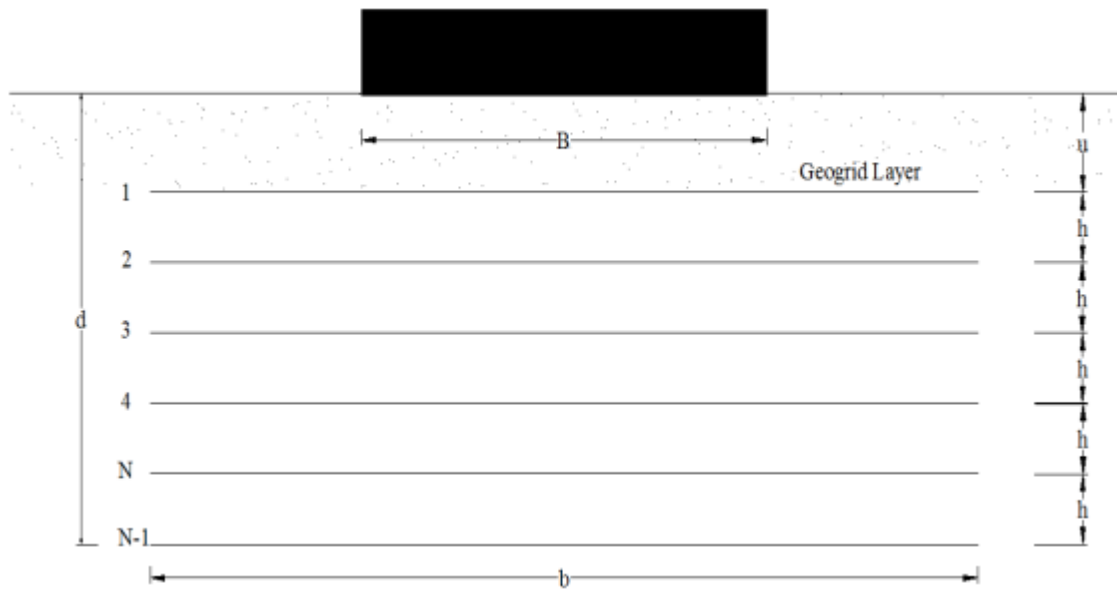


Fig 4.1 placement of geogrid layers



Fig 4.2 placement of geogrid in the tank

### 4.3 TEST PROCEDURE

- At first, the test tank is filled from the desired height, by rain falling technique, and it is leveled by means of a scale. And the footing is placed at desired location over the sand fill to transfer the load vertically.
- Then the grooving metallic ball is placed on the depression of centre or eccentric position, according to different loading conditions, then the load transferring shaft is placed over it, through which the load is transferred to the footing.
- Two dial gauges are placed on the surface of the footing on the opposite sides of it. Then the initial readings of two dial gauges are noted, and as the load is increased, the readings are noted down.
- The load is applied gradually in an increasing manner and the footing is allowed to settle under the applied load. The load increment is maintained until the footing settlement gets stabilized which is measured from the two dial gauge readings until the pointer halts.
- The footing is loaded at a constant incremental loading rate until an ultimate bearing state was reached. The ultimate bearing state is defined as reached, as the state in which either the load reached a maximum value where the settlements continued without any further increase in load or if there is a sudden change in the load vs settlement relationship which can be observed from the load –settlement data.
- Before the start of a new test, the sand in the test tank is emptied out, from the previous test to a depth of about  $3B$ , where  $B$  is the width of the footing, and deeper for multilayer reinforcements.



Fig 4.3 Equipment set up

#### 4.4 MODEL TEST SERIES

Number of Test	Number of Geogrid Layers ( $N$ )	Depth of embedment ( $D_f/B$ )	$B/L$	$e/B$
1-4	0	0.5	1	0,0.05,0.10,0.15
4-8	0	1.0	1	0,0.05,0.10,0.15
8-12	2	0.5	1	0,0.05,0.10,0.15
12-16	3	0.5	1	0,0.05,0.10,0.15
16-20	4	0.5	1	0,0.05,0.10,0.15
20-24	2	1.0	1	0,0.05,0.10,0.15
24-28	3	1.0	1	0,0.05,0.10,0.15
28-32	4	1.0	1	0,0.05,0.10,0.15

## RESULTS AND DISCUSSIONS

### 5.1 General

A number of experiments are performed on model square footing of size  $10\text{cm} \times 10\text{cm} \times 3\text{cm}$ , with eccentricity varying from 0 to  $0.15B$ , resting on unreinforced as well as reinforced granular bed. Reinforced sand bed, with multiple number (2, 3, 4) of geogrid (TGB40) layers are placed for the fill. As the load is increased gradually, the settlement corresponding to it, is noted down and the results are plotted in the form of load vs settlement curve. Load carrying capacity for each test of varied condition is found out from the curve using double tangent intersection method.

### 5.2 MODEL TESTS

#### 5.2.1 RESULTS BEARING CAPACITY OF UNREINFORCED SAND

Results are observed from the load vs settlement curve as shown in the figures below. From the graphs, keen observations have been made to reach the conclusions of the behavior of the square footing on the unreinforced sand bed, and their different characteristics.

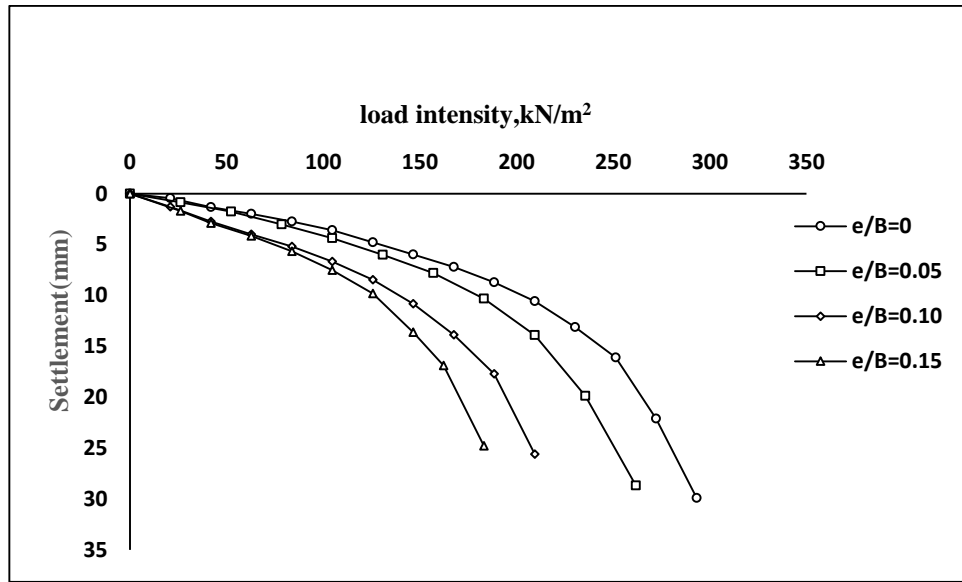


Fig 5.1 Load vs settlement curve for  $D_f/B=0.5$  &  $N=0$  and different  $e/B$  ratios

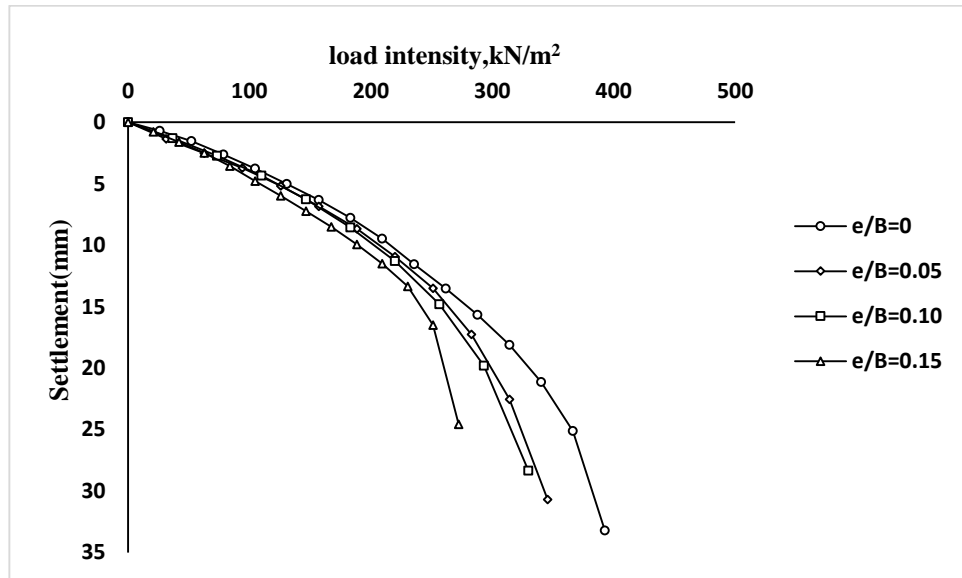


Fig 5.2 Load vs settlement curve for  $D_f/B=1.0$  &  $N=0$  and different  $e/B$  ratios

From the Load vs settlement curves, as shown in the above figures, ultimate load carrying capacity of both  $D_f/B$  ratio i.e. 0.5 & 1.0 and for centric & varied eccentricities i.e. 0.05B, 0.10B, 0.15B have been calculated using double tangent intersection method.



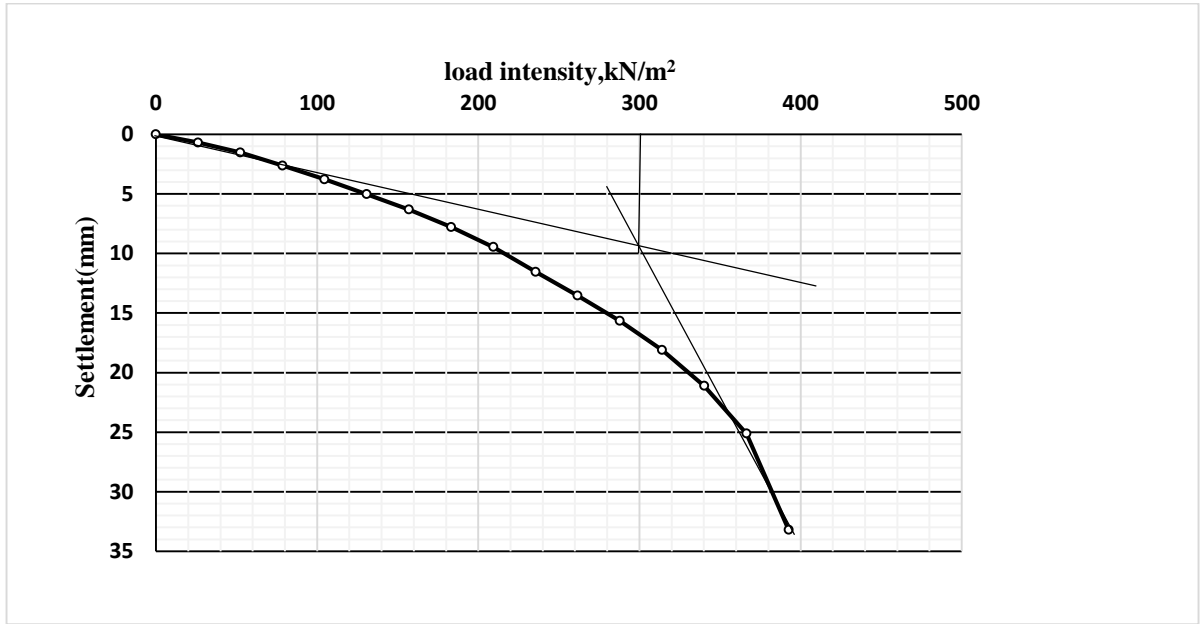


Fig 5.3 Calculation of ultimate bearing capacity by tangent intersection method

Here, a tangent is drawn from the start point of the curve, and a tangent is drawn from the end point of the curve, and the point ,where they intersect, gives the load carrying capacity point.

Table 5.1 Comparison of load carrying capacity values with the experimental ones

$D_f/B$	N	$e/B$	experimental, $q_u$ (kN/m <sup>2</sup> )	theoretical, $q_u$ (kN/m <sup>2</sup> )
0.5	0	0.00	230	126
		0.05	196	105.95
		0.10	168	91.03
		0.15	138	77.60
1.0	0	0.00	300	178
		0.05	280	155
		0.10	250	136
		0.15	230	118

### 5.2.1 BEARING CAPACITY OF REINFORCED SAND BED

Model tests are performed on square footing of dimension, 10cmx10cmx3cm on geogrid reinforced sand. The multilayered geogrid reinforced layers are varied with 2, 3 or 4 in number. The embedment depth is varied as 0.5B and 1.0B from the surface of the footing. And the footing is subjected to centric and different eccentricities 0.5B, 0.10B, and 0.15B. The settlement corresponding to increasing load is plotted on graph, and by tangent intersection method, the ultimate load is obtained from the graph, for various conditions.

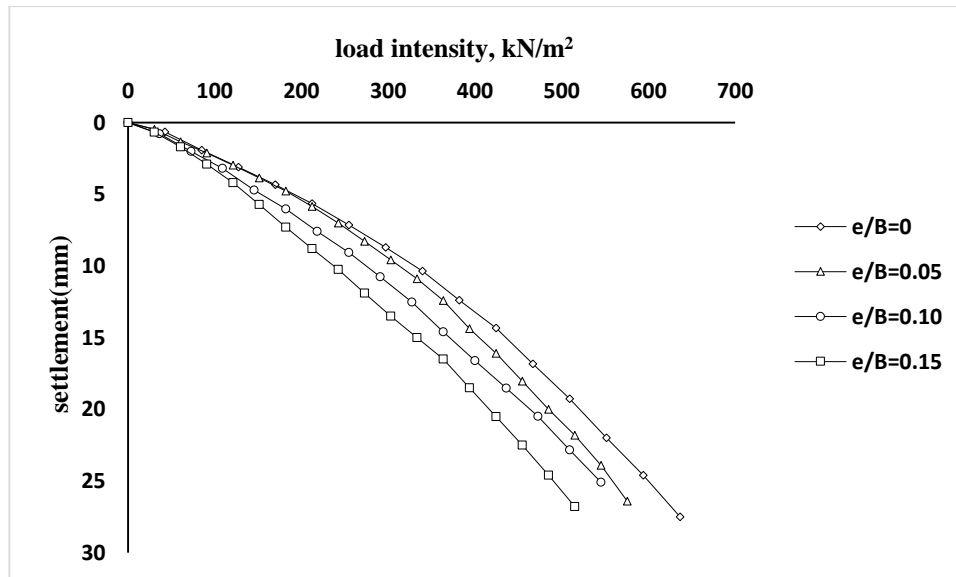


Fig 5.3 Load vs settlement curve for  $D_f/B=0.5$  &  $N=2$  for different  $e/B$  ratios

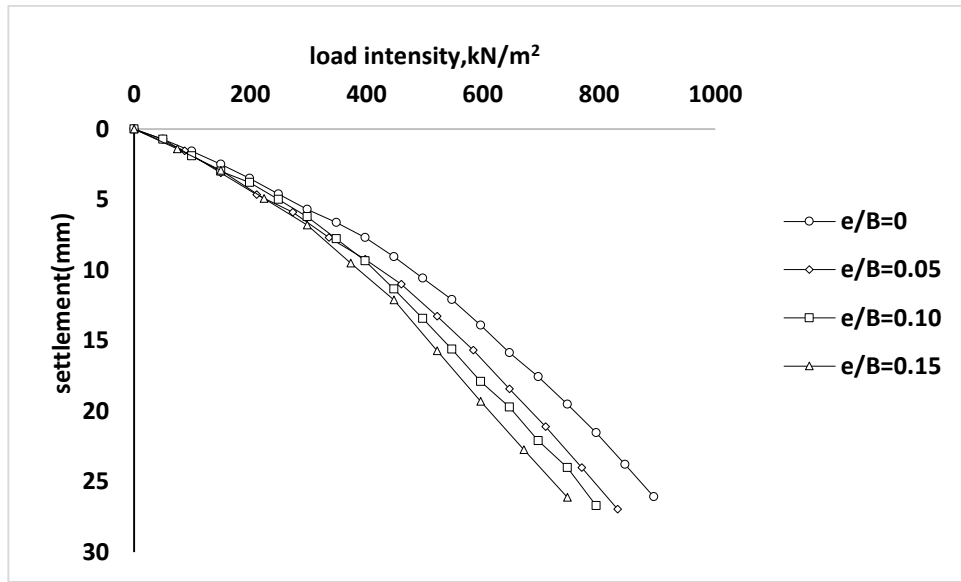


Fig 5.5 Load vs settlement curve for  $D_f/B=0.5$  &  $N=3$  for different  $e/B$  ratios

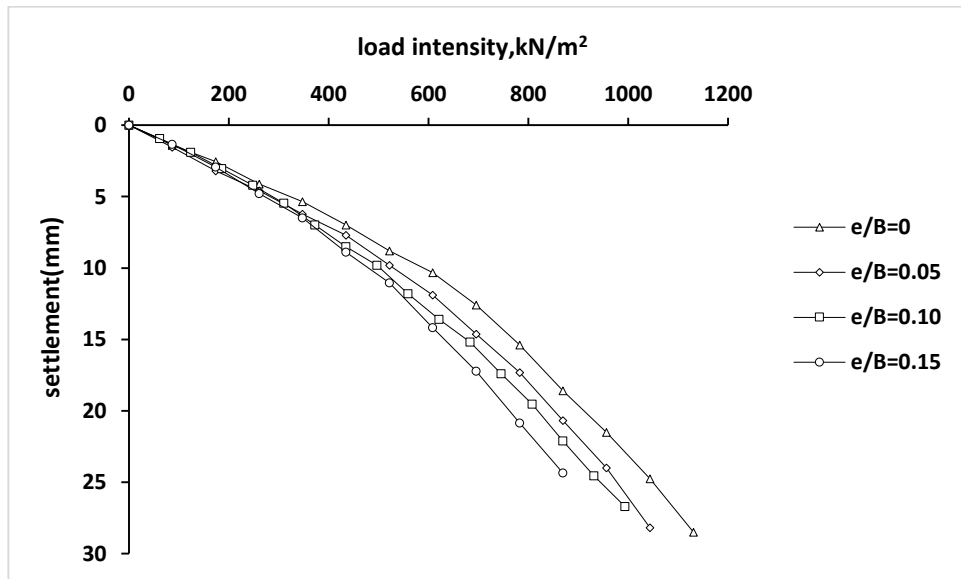


Fig 5.6 Load vs settlement curve for  $D_f/B=0.5$  &  $N=4$  for different  $e/B$  ratios

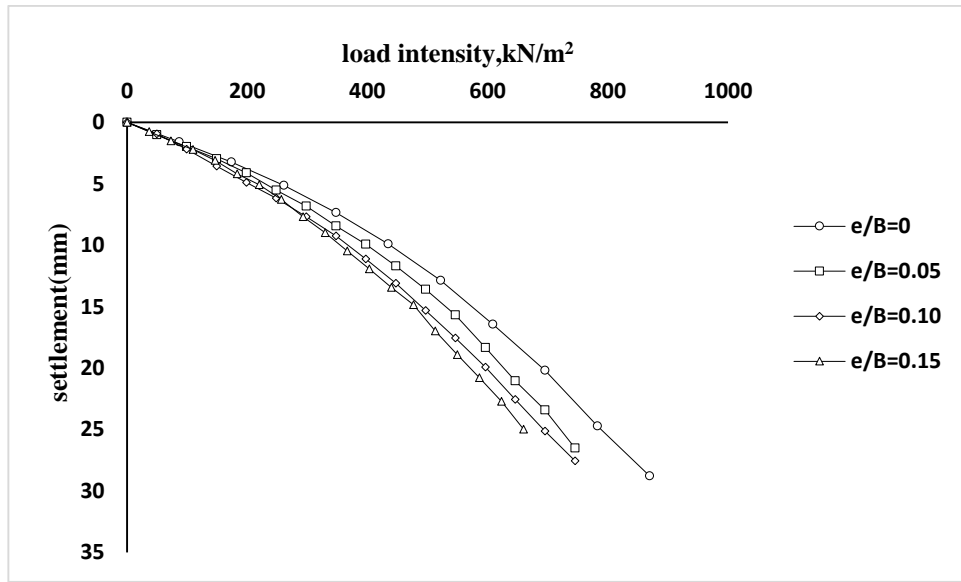


Fig 5.7 Load vs settlement curve for  $D_f/B=1.0$  &  $N=2$  for different  $e/B$  ratios

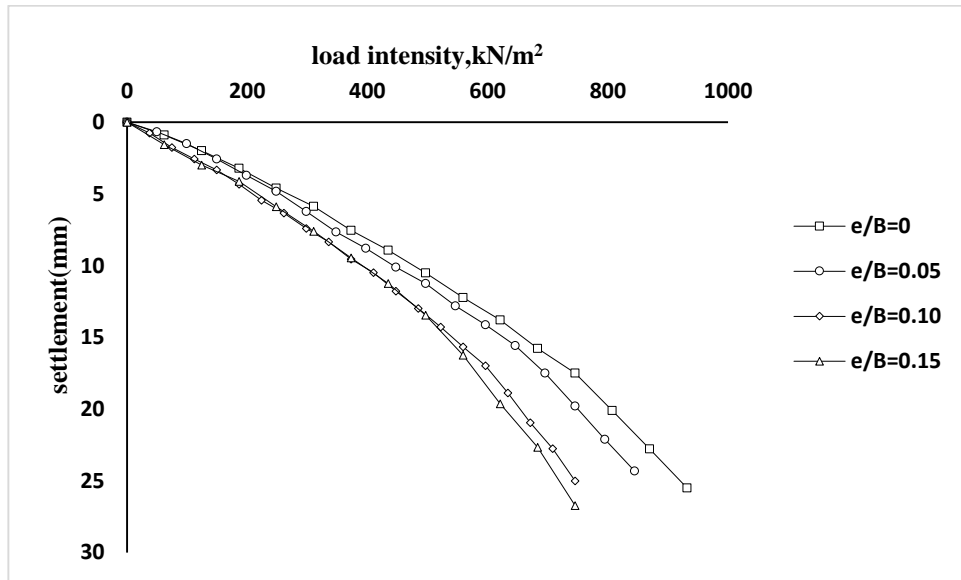


Fig 5.8 Load vs settlement curve for  $D_f/B=1.0$  &  $N=3$  for different  $e/B$  ratios

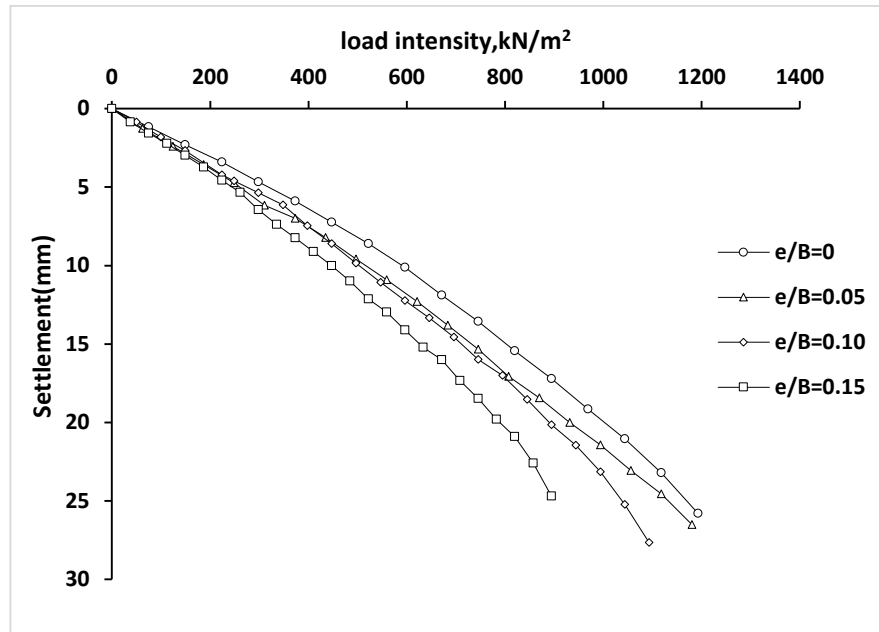


Fig 5.9 Load vs settlement curve for  $D_f/B=1.0$  &  $N=4$  for different  $e/B$  ratios

From the above graphs, we can see that, as the  $e/B$  ratio increases, the bearing capacity decreases.

**Comparison of load – Settlement graphs of same eccentricities with varying geogrid layers.**

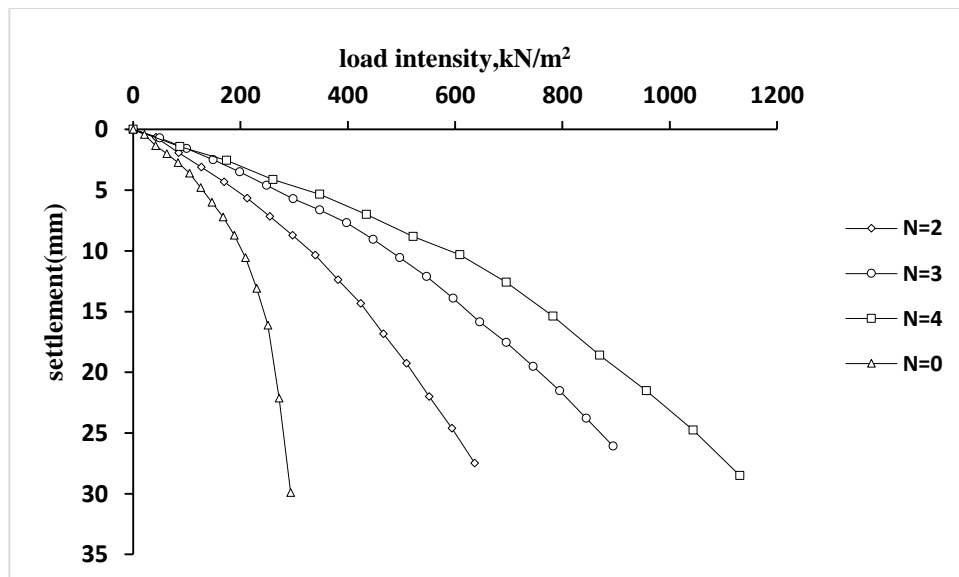


Fig 5.10 Load vs settlement curve for  $D_f/B=0.5$  &  $e/B=0$  for different  $N$  layers

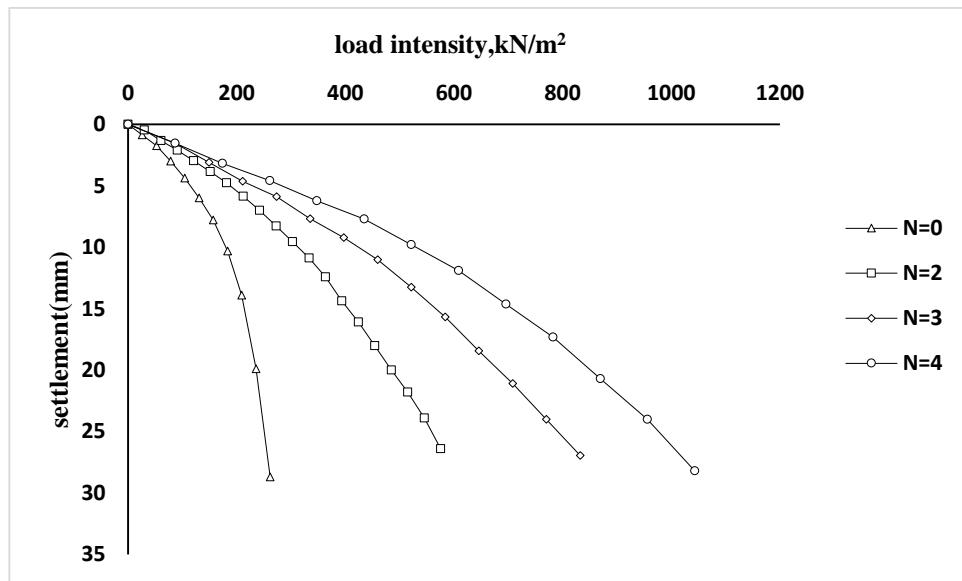


Fig 5.11 Load vs settlement curve for  $D_f/B=0.5$  &  $e/B=0.05$  for different  $N$  layers

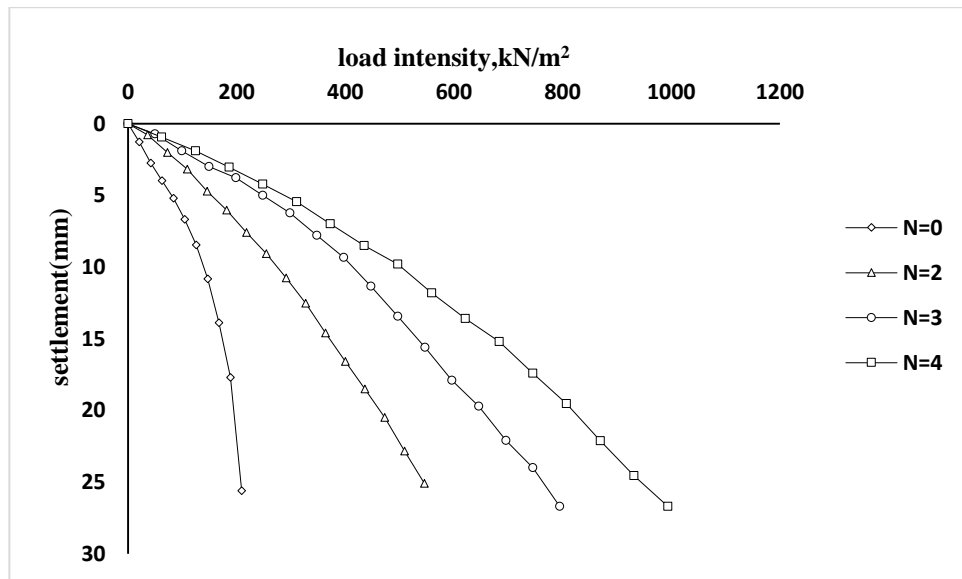


Fig 5.12 Load vs settlement curve for  $D_f/B=0.5$  &  $e/B=0.10$  for different  $N$  layers

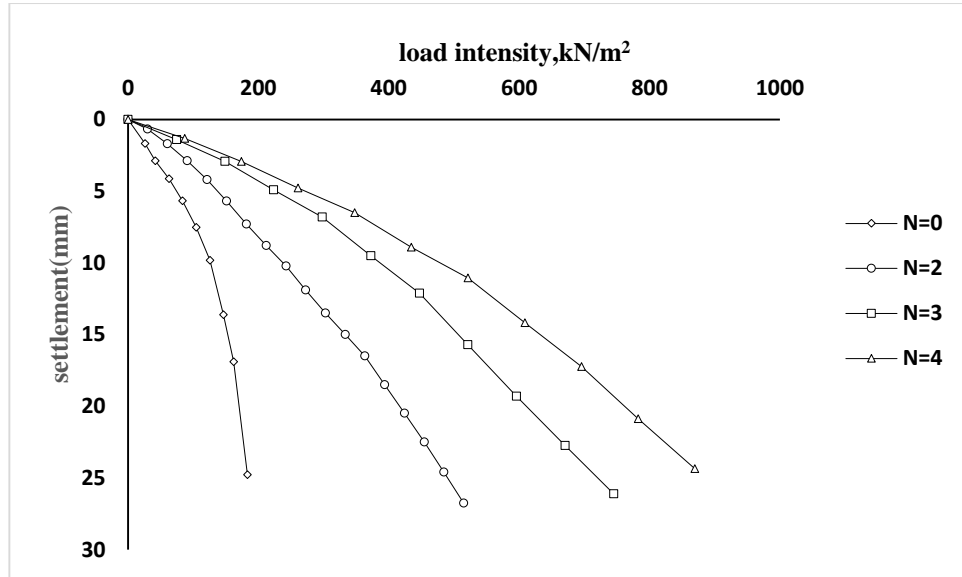


Fig 5.13 Load vs settlement curve for  $D_f/B=0.5$  &  $e/B=0.15$  for different  $N$  layers

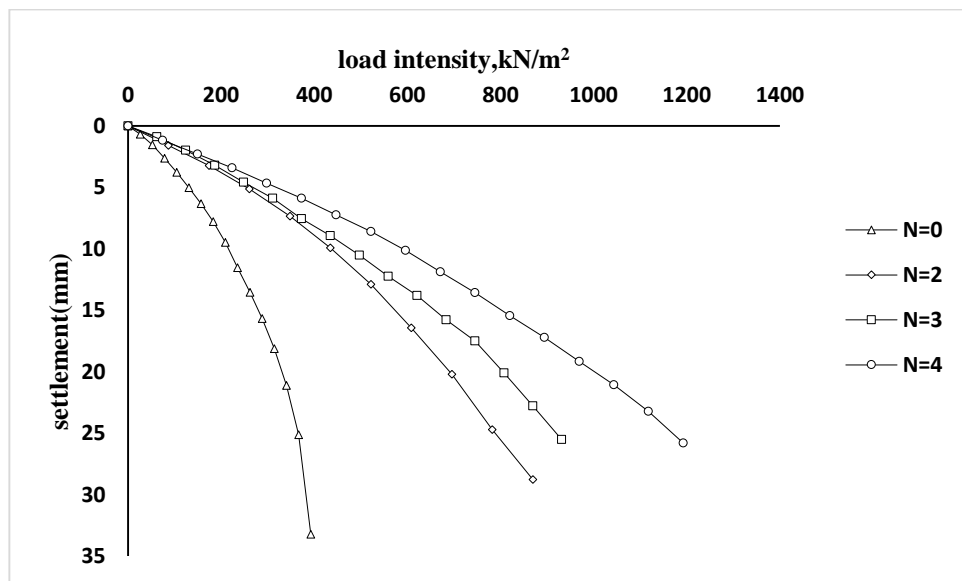


Fig 5.14 Load vs settlement curve for  $D_f/B=1.0$  &  $e/B=0$  for different  $N$  layers

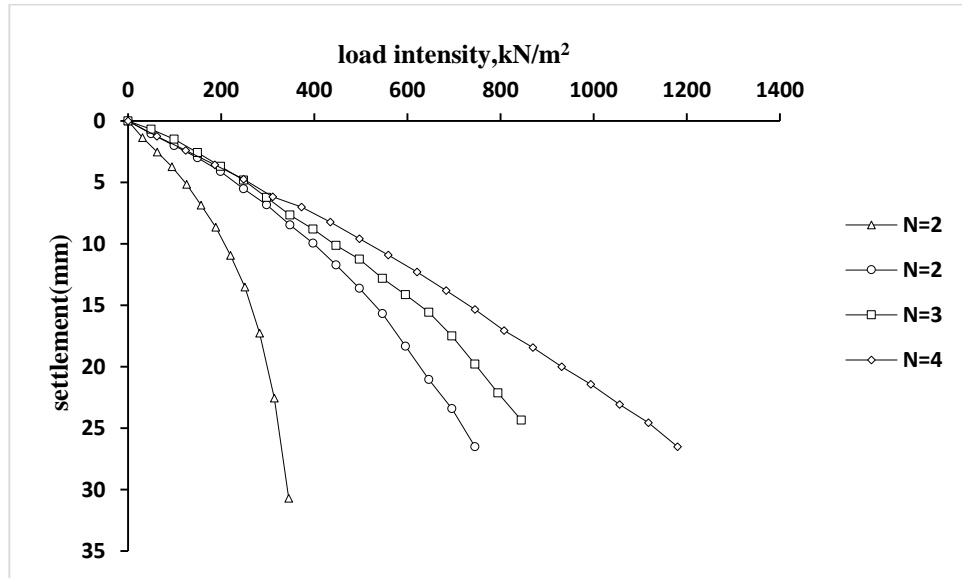


Fig 5.15 Load vs settlement curve for  $D_f/B=1.0$  &  $e/B=0.05$  for different  $N$  layers

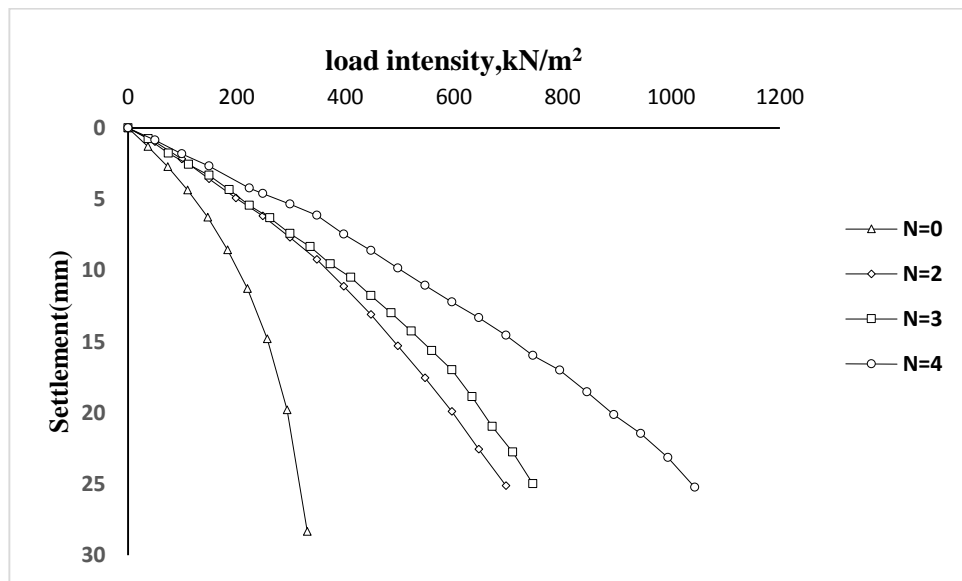


Fig 5.16 Load vs settlement curve for  $D_f/B=1.0$  &  $e/B=0.10$  for different  $N$  layers



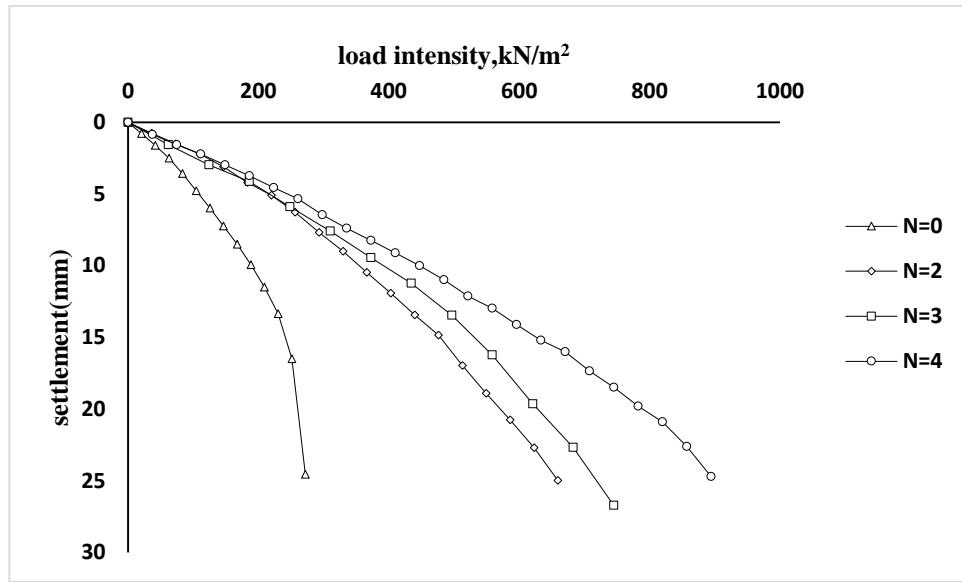


Fig 5.17 Load vs settlement curve for  $D_f/B=1.0$  &  $e/B=0.15$  for different  $N$  layers

By observing the above graphs, we can say that, as the number of geogrid layer increases ,load carrying capacity also increases

**Load –Settlement curves of footing of same eccentricities and same number of geogrid layers with varying embedment depth**

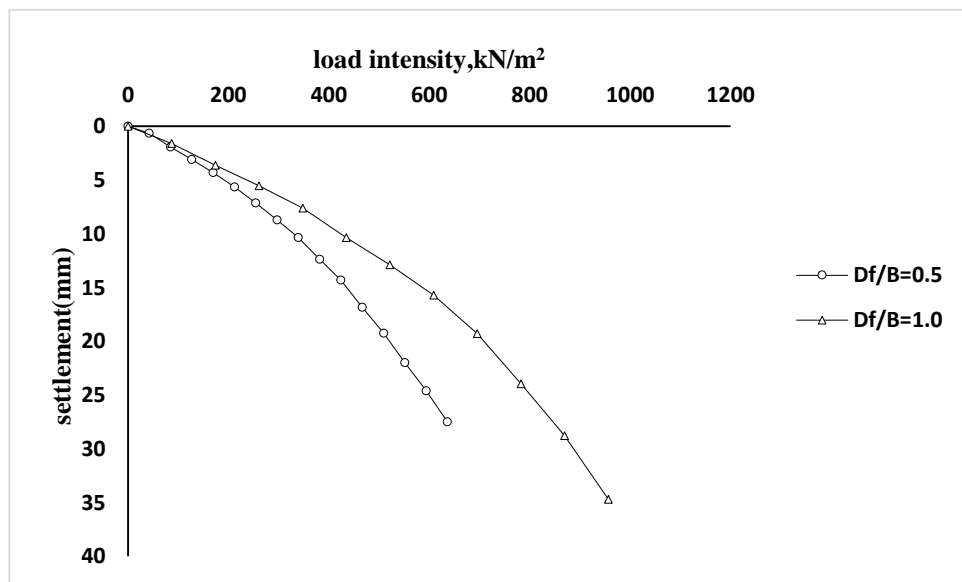


Fig 5.18 Load vs settlement curve for  $N=2$  &  $e/B=0$  for different  $D_f/B$  depths

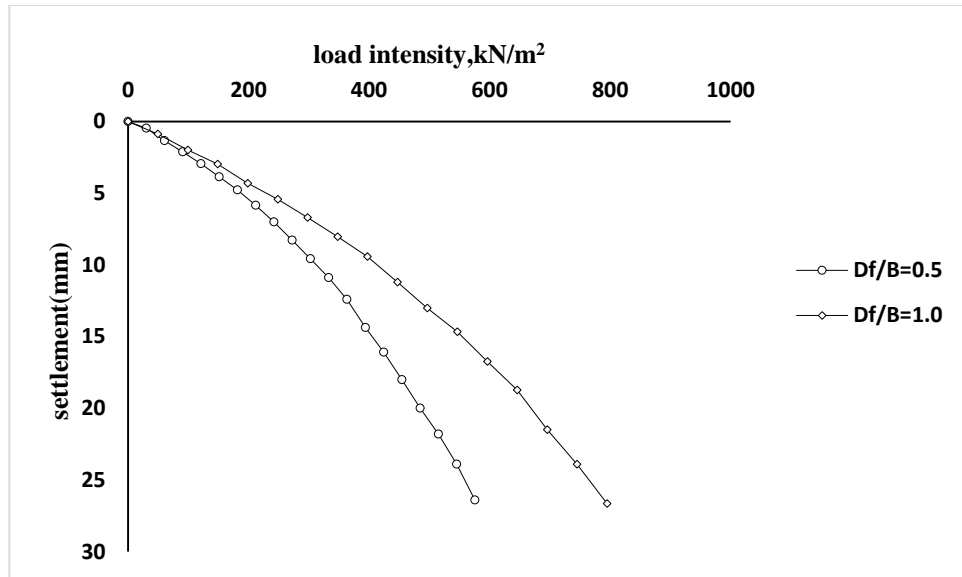


Fig 5.19 Load vs settlement curve for  $N=2$  &  $e/B=0.05$  for different  $D_f/B$  depths

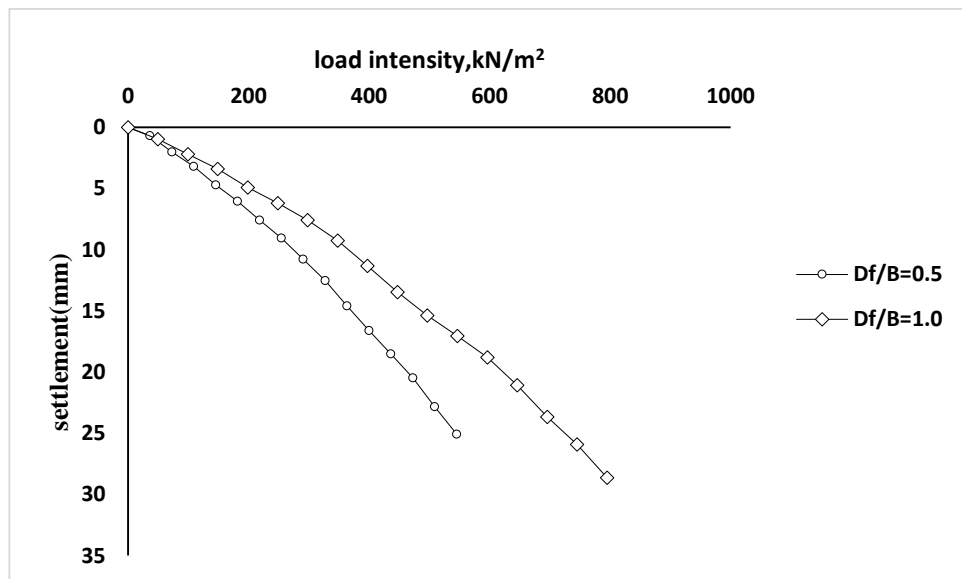


Fig 5.20 Load vs settlement curve for  $N=2$  &  $e/B=0.10$  for different  $D_f/B$  depths

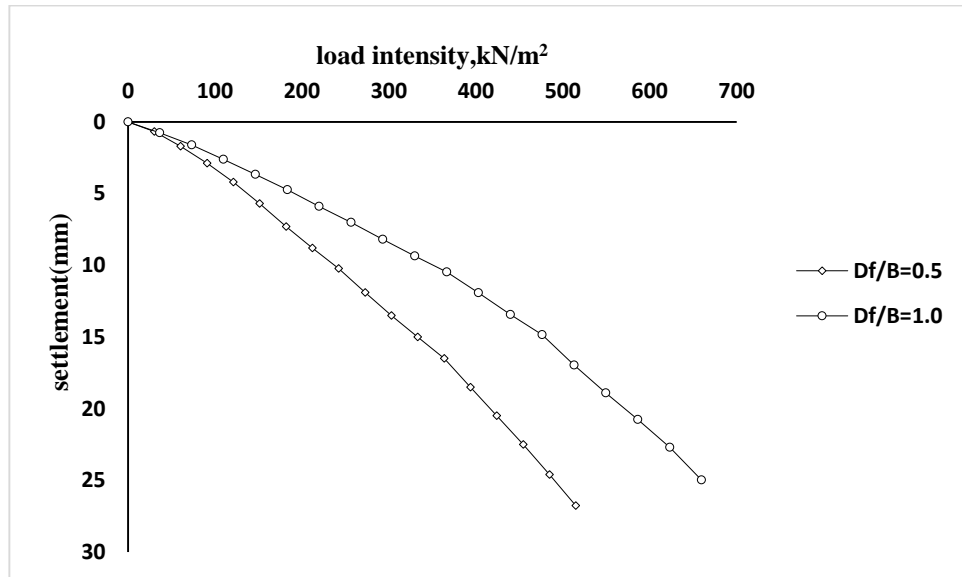


Fig 5.21 Load vs settlement curve for  $N=2$  &  $e/B=0.15$  for different  $D_f/B$  depths

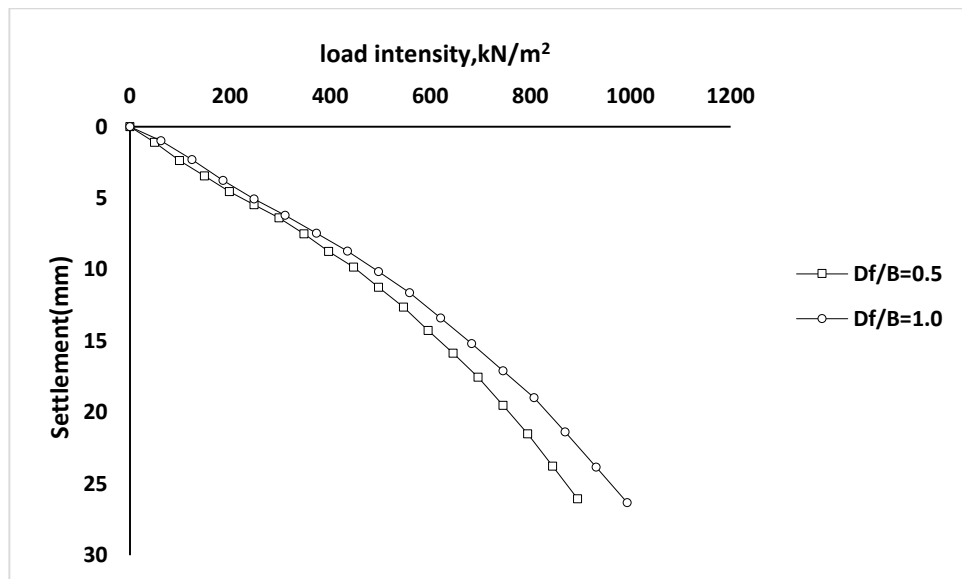


Fig 5.22 Load vs settlement curve for  $N=3$  &  $e/B=0$  for different  $D_f/B$  depth

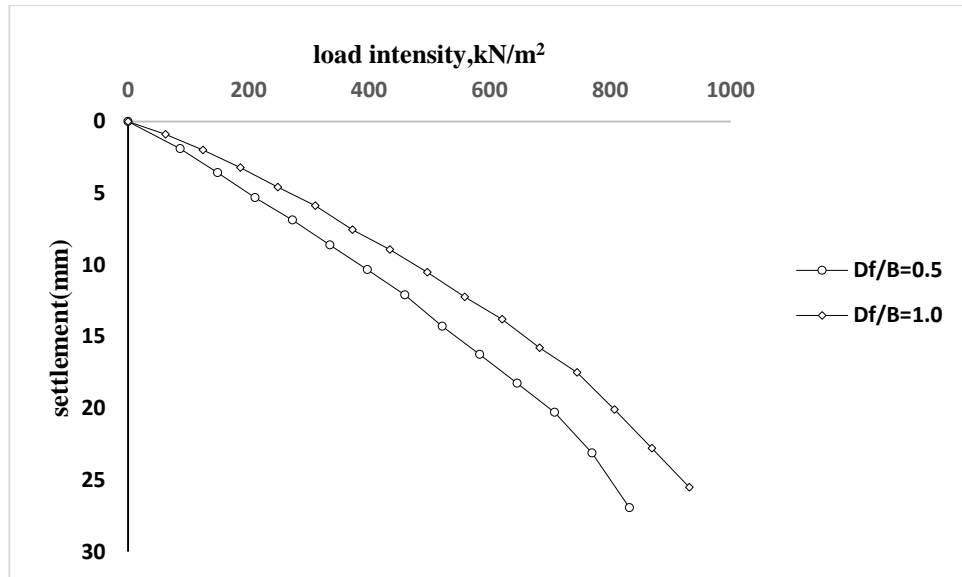


Fig 5.23 Load vs settlement curve for  $N=3$  &  $e/B=0.05$  for different  $D_f/B$  depth

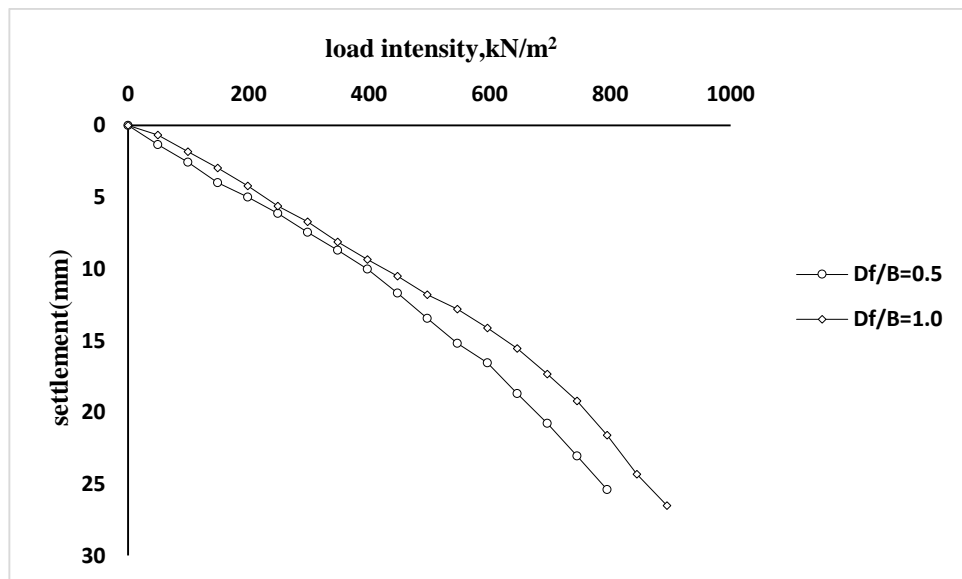


Fig 5.24 Load vs settlement curve for  $N=3$  &  $e/B=0.10$  for different  $D_f/B$  depth

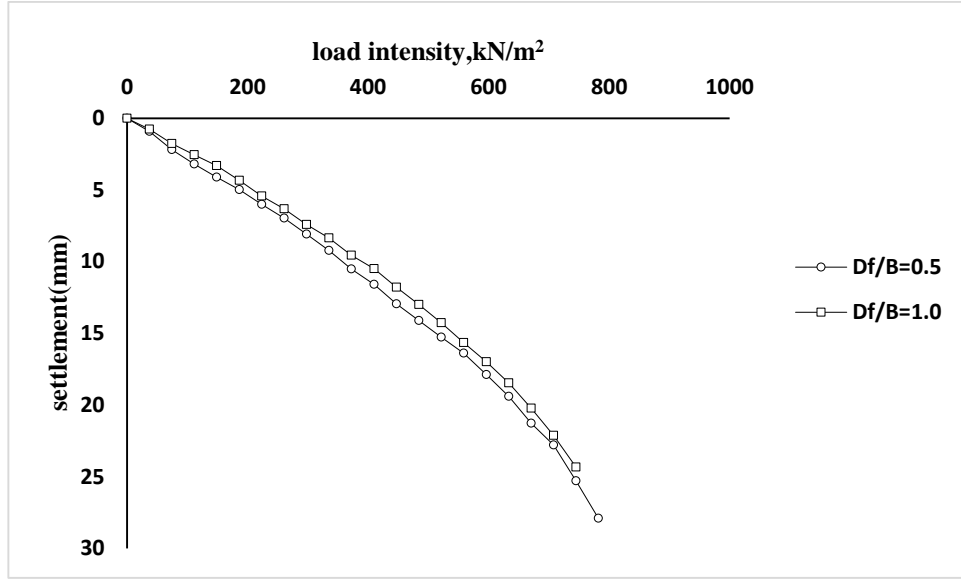


Fig 5.25 Load vs settlement curve for  $N=3$  &  $e/B=0.15$  for different  $D_f/B$  depth

By observing the above graphs, we can say that, as the embedment depth increases, load carrying capacity also increases.

Theoretical bearing capacity for reinforced case is given by Huang and Menq in 1997 for strip footing, which was later added by a shape factor, given as,

$$q_u = \left[ 0.5 - 0.1 \left( \frac{B}{L} \right) \right] (B + \Delta B) \gamma N_\gamma + D_f N_q \quad (5.1)$$

The above one, gives the bearing capacity for centrally loaded footing, for eccentric cases, a reduction factor, as proposed by Purkayastha and Char in 1977 for unreinforced conditions has been extended. The reduction factor is given by,

$$q_{uR(e)} = q_{uR(e=0)} (1 - R_k) \quad (5.2)$$

Here,  $q_{uR(e)}$  is the bearing capacity for reinforced sand under eccentric loading, and is the bearing capacity of reinforced sand under centric loading. The reduction factor,  $R_k$  used here is, as proposed by, Patra et al.

$$R_k = 4.97 \left( \frac{df}{B} \right)^{-0.21} \left( \frac{e}{B} \right)^{1.21} \quad (5.3)$$

## 5.3 ANALYSIS OF RESULTS

Here graph analysis is used to find out a generalized empirical correlation to find out the bearing capacity of the eccentric loaded footing, if the bearing capacity of centric loaded footing is known. The load carrying capacity values of reinforced and unreinforced sand of both cases i.e  $D_f/B=0.5$  and  $1.0$  with different values of  $e/B$  and  $N$  is enlisted in Table 5.2 and Table 5.3. Using the experimental load carrying capacity values, as calculated from Load vs settlement curves, the ratio  $q_{UR}(e)/q_{UR}$  has been calculated for each case of different reinforcement depths. Then the experimental  $R_{kR}$  is found out and the deviation of it from the predicted is found out. The reduction factor  $R_{kR}$  is then calculated for each case by using equation 5.2 and tabulated in Table 5.2 and Table 5.3.

An empirical relation for reduction factor ( $R_{kR}$ ), as proposed by Patra et al. (2006) for strip footing shows that  $R_{kR}$  is the function of  $d_f/B$  and  $e/B$ ,

$$R_k = \alpha_1 \left( \frac{d_f}{B} \right)^{\alpha_2} \left( \frac{e}{B} \right)^{\alpha_3} \quad (5.4)$$

where  $\alpha_1, \alpha_2, \alpha_3$  are dimensionless constants.

Here the coefficient values of  $\alpha_1, \alpha_2, \alpha_3$  for the square footing is found out by conducting a number of laboratory model tests using square footing with embedment depth as  $D_f/B=0.5$  and  $1.0$  resting over multi-layered geogrid reinforced sand bed through this analysis.

### 5.3.1 Analysis of square footing for $D_f/B=0.5$

At first, the value of  $\alpha_3$  is found out from the graph, as plotted  $R_{kR}$  vs  $e/B$  curve as shown in the Figure 5.27 and  $\alpha_2$  is found out using  $R_{kR}$  vs  $d_f/B$  curve, as plotted on log-log graph as shown in Figure 5.26.

Table 5.2 Experimental reduction factor for eccentrically loaded footing resting on reinforced sand bed with  $D_f/B=0.5$

<b>N</b>	<b>e/B</b>	<b>d<sub>f</sub>/B</b>	<b>Theoretical <math>q_u</math></b>	<b>Experimental <math>q_u</math></b>	<b>Expt. <math>RF</math></b>	<b><math>R_{KR}</math></b>
0	0	0.5	126.08	230	1.00	0.00
	0.05		105.95	196	0.85	0.15
	0.1		91.03	168	0.73	0.27
	0.15		77.6	138	0.60	0.40
2	0	1.1	224.31	350	1.00	0.00
	0.05		195.19	318	0.91	0.09
	0.1		156.93	278	0.79	0.21
	0.15		114.27	239	0.68	0.32
3	0	1.35	265.24	495	1.00	0.00
	0.05		232.25	445	0.90	0.10
	0.1		188.92	385	0.78	0.22
	0.15		140.59	331	0.67	0.33
4	0	1.6	306.16	680	1.00	0.00
	0.05		268.91	605	0.89	0.11
	0.1		221.15	519	0.76	0.24
	0.15		167.32	441	0.65	0.35

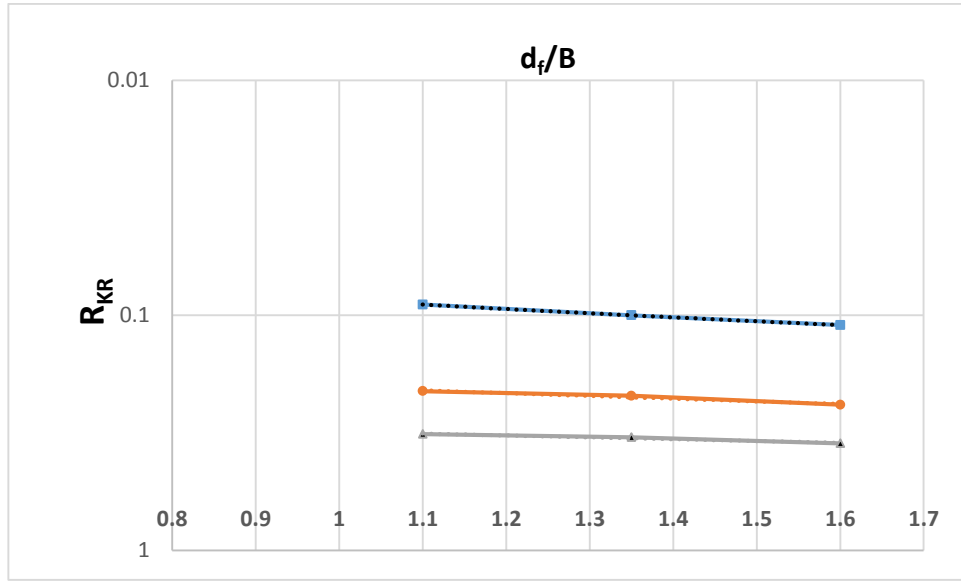


Fig 5.26 Variation of  $R_{KR}$  with  $d_f/B$  for  $D_f/B=0.5$

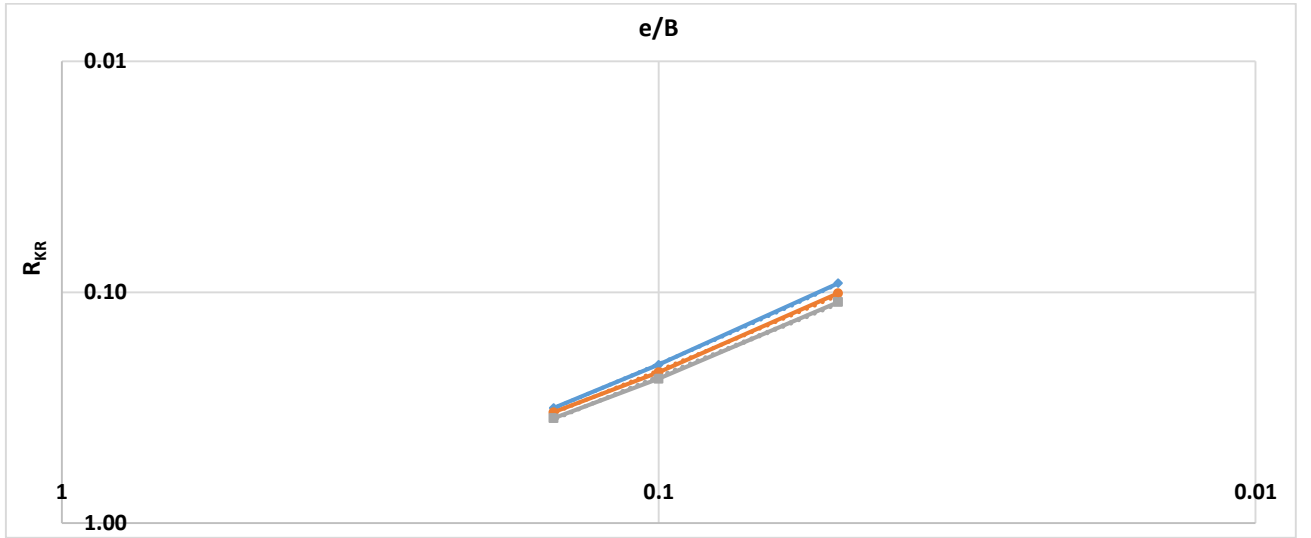


Figure 5.27 Variation of  $R_{KR}$  with  $e/B$  for  $D_f/B=0.5$

From the above Figure 5.27, we found out the slope of the line having maximum coefficient of correlation is found out. The value of  $\alpha_3$  has been found as 1.11.

$$R_{KR} \propto \left(\frac{e}{B}\right)^{1.11} \quad (5.5)$$



From the above Figure 5.26, we found out the slope of the line having maximum coefficient of regression is found out. The value of  $\alpha_2$  has been found out as 0.04.

$$R_{KR} \propto \left(\frac{d_f}{B}\right)^{0.04} \quad (5.6)$$

By combining both the Equations 5.5 and 5.6, the reduction factor as shown in equation 5.4 may be written as

$$R_{KR} = \alpha_1 \left(\frac{d_f}{B}\right)^{0.04} \left(\frac{e}{B}\right)^{1.11} \quad (5.7)$$

Now for the calculation of  $\alpha_1$ , graph is plotted by  $e/B$  ratio for each  $d_f/B$ , reinforcement depth and corresponding  $R_{KR}$  value by using Equation 5.5 and then the average value is taken as  $\alpha_1$ .

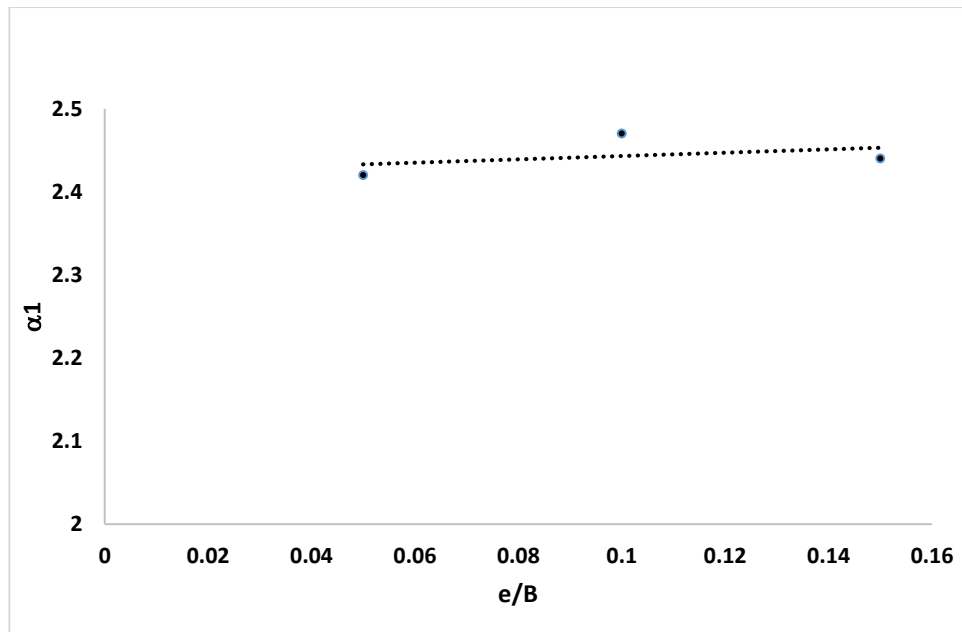


Fig 5.28 Variation of  $\alpha_1$  with  $e/B$  for  $D_f/B=0.5$

The average value of  $\alpha_1$  from the Figure 5.28 has been found out as 2.77. And the final equation may be written for  $D_f/B=0.5$  can be written as shown in equation 5.8

$$R_k = 2.77 \left(\frac{d_f}{B}\right)^{0.04} \left(\frac{e}{B}\right)^{1.11} \quad (5.8)$$

### 5.3.2 Analysis of square footing with $D_f/B = 1.0$

At first, the value of  $\alpha_3$  is found out from the graph, as plotted  $R_{KR}$  vs  $e/B$  curve as shown in the Figure 5.30 and  $\alpha_2$  is found out using  $R_{KR}$  vs  $d_f/B$  curve, as plotted on log-log graph as shown in Figure 5.29

Table 5.3 Experimental reduction factor for eccentrically loaded footing resting on reinforced sand bed with  $D_f/B=1.0$

<b>Z</b>	<b>e/B</b>	<b>d<sub>f</sub>/B</b>	<b>Theoretical <math>q_u</math></b>	<b>Experimental <math>q_u</math></b>	<b>Expt. RF</b>	<b><math>R_{KR}</math></b>
0	0	1.0	178.62	300	1.00	0.00
	0.05		155.85	280	0.93	0.07
	0.1		136.55	250	0.83	0.17
	0.15		118.31	230	0.77	0.23
2	0	1.6	276.6	460	1.00	0.00
	0.05		243.46	421	0.92	0.08
	0.1		200.63	381	0.83	0.17
	0.15		151.17	329	0.72	0.28
3	0	1.85	317.5	610	1.00	0.00
	0.05		280.64	556	0.91	0.09
	0.1		232.07	491	0.80	0.20
	0.15		177.97	419	0.69	0.31
	0		358.39	785	1.00	0.00
	0.05		317.78	710	0.90	0.10

4	0.1	2.1	264.4	610	0.78	0.22
	0.15		204.88	541	0.69	0.31

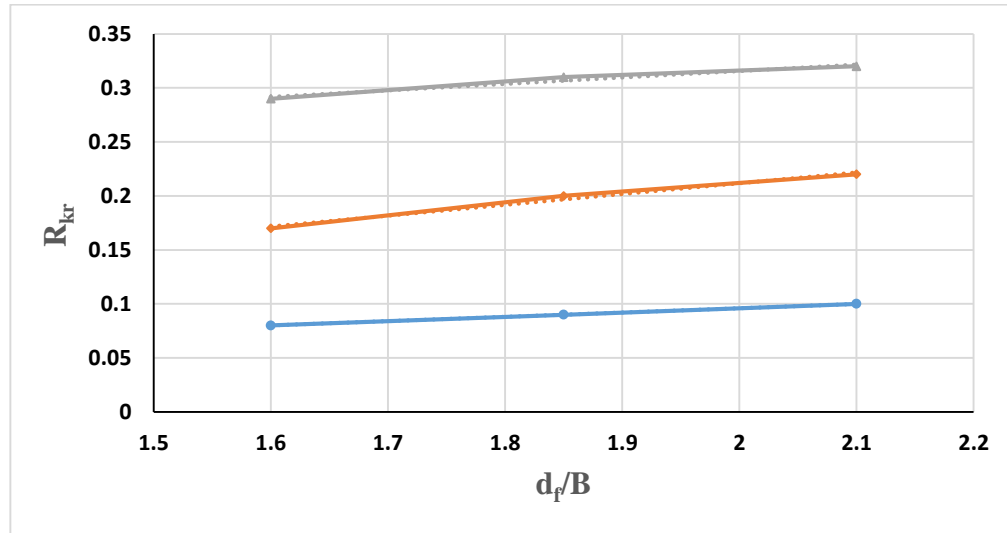


Fig 5.29 Variation of  $R_{KR}$  with  $d_f/B$  for  $D_f/B=1.0$

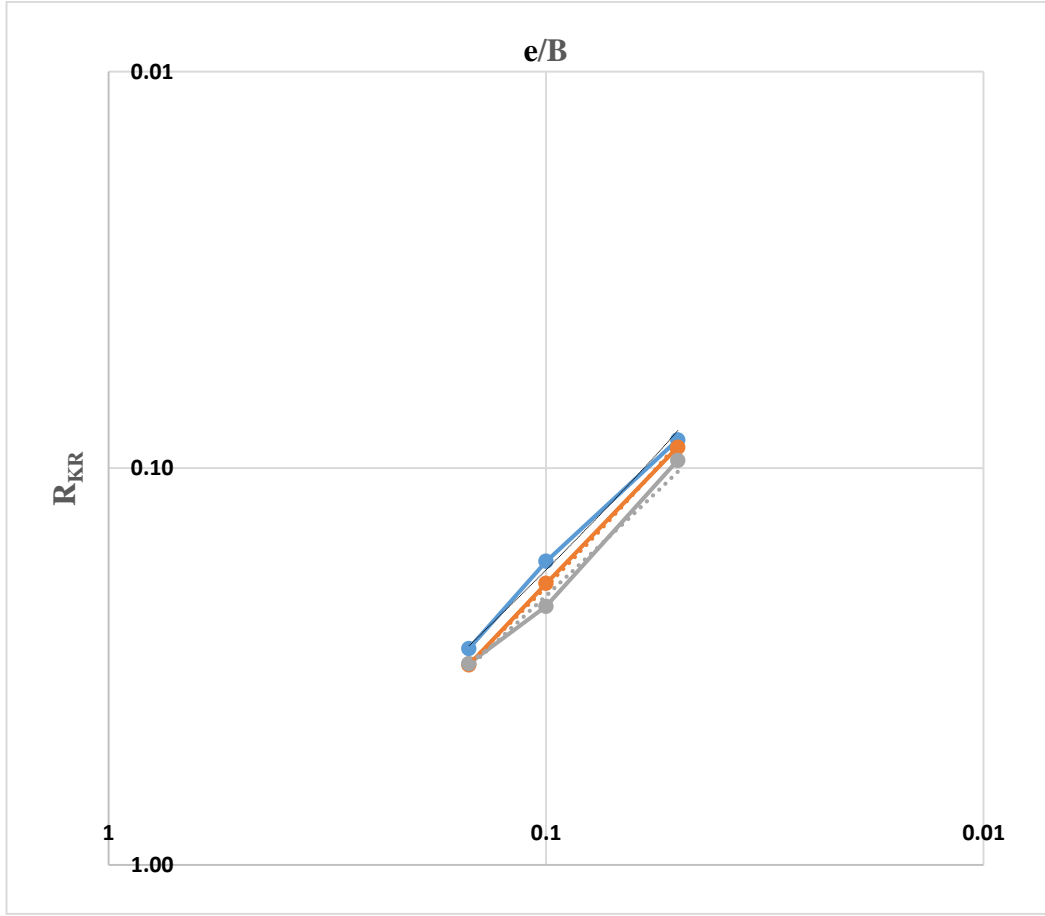


Figure 5.30 Variation of  $R_{KR}$  with  $e/B$  for  $D_f/B=1.0$

From the above Figure 5.27, we found out the slope of the line having maximum coefficient of correlation is found out. The value of  $\alpha_3$  has been found as 1.12.

$$R_{KR} \propto \left(\frac{e}{B}\right)^{1.12} \quad (5.9)$$

By combining both the Equations 5.5 and 5.6, the reduction factor as shown in Equation 5.4 may be written as

$$R_{KR} \propto \left(\frac{d_f}{B}\right)^{0.04} \quad (5.10)$$

By combining Equation 5.9 and 5.10, equation for reduction factor as shown in Equation 5.4 may be written as

$$R_k = \alpha_I \left( \frac{df}{B} \right)^{0.04} \left( \frac{e}{B} \right)^{1.12} \quad (5.11)$$

Now the value of  $\alpha_I$  will be calculated for each  $e/B$  ratio and one  $df/B$  and corresponding  $R_{KR}$  value by using Equation 5.7 and then the average value is taken as  $\alpha_I$ .

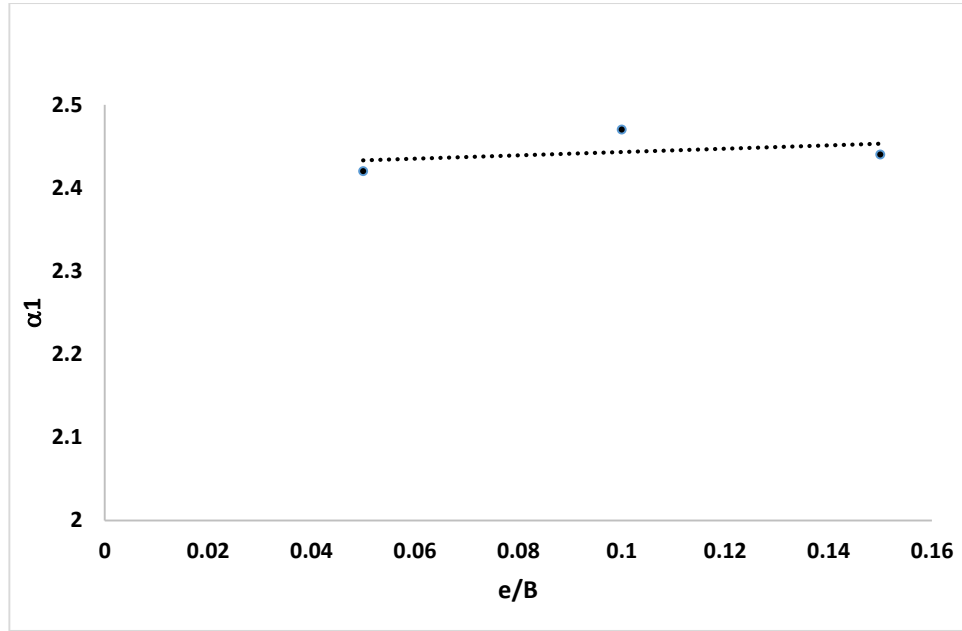


Fig 5.31 Variation of  $\alpha_I$  with  $e/B$  for  $D_f/B=1.0$

By combining Equation 5.9 and 5.10, equation for reduction factor as shown in equation 5.11 may be written as

$$R_k = 2.44 \left( \frac{df}{B} \right)^{0.04} \left( \frac{e}{B} \right)^{1.12} \quad (5.12)$$

## CONCLUSION

In this present work, bearing capacity of square footing subjected to centric and eccentric loading, reinforced under multilayer geogrids, with different embedment depths is found out.

From the current research work, we can conclude that,

- As the load shifts from centric to eccentric one, bearing capacity of granular medium decreases.
- As the number of geogrid layer increases, the bearing capacity increases.
- The bearing capacity also increases with the embedment depth.
- An empirical equation for reduction factor has been developed to determine the bearing capacity of square footing under eccentric load resting on reinforced sand by knowing the bearing capacity of centric load at same condition.

## REFERENCES

1. Basudhar, P. K., Dixit, P. M., Gharpure, A., Deb, K. (2008). "Finite element analysis of geotextile-reinforced sand-bed subjected to strip loading." *Geotextiles and Geomembranes*, 26, pp. 91-99.
2. Behera, R. N. (2012). "Behaviour of shallow strip foundation on granular soil under eccentrically inclined load." *Ph.D Thesis*, NIT Rourkela.
3. Dash, S. K., Krishnaswamy, N. R., Rajagopal, K. (2001). "Bearing capacity of strip footings supported on geocell-reinforced sand." *Geotextiles and Geomembranes*, 19, pp. 235-256.
4. Das, B. M., Omar, M. T. (1994). "The effect of foundation width on model tests for the bearing capacity of sand with geogrid reinforcement." *Geotechnical and Geological Engineering* 12, pp133-141.
5. Das, B. M., Shin, E. C., Omar, M. T. (1994). "The bearing capacity of surface strip foundations on geogrid-reinforced sand and clay – a comparative *Geotechnical and Geological Engineering* 12, pp1-14.
6. Das, B. M., "Shallow Foundation, Second Edition." *CRC Press*.
7. Das, B. M., "Principles of Foundation Engineering, Seventh Edition." *CENGAGE Learning*.
8. DeBeer, E. E. (1970), "Experimental determination of the shape factors of sand." *Geotechnique*. 20(4): 307.
9. Farah, C. A., "Load carrying capacity of Shallow Foundations on Layered Soil." *A Thesis in the Department of Building, Civil and Environmental Engineering, Concordia*

University, Canada.

10. GEOGRIDS, *Geosynthetics Specifier's Guide 2012*

11. Hansen, J. B. (1970). "A revised and extended formula for bearing capacity." Bulletin No. 28, *Danish Geotechnical Institute, Copenhagen*.

12. Hight W. H., Anders J. C. (1985) . "Dimensioning Footing Subjected to Eccentric Load." *Journal of Geotechnical Engineering* Vol 111, No.5.

13. Huang, C.C., and Menq, F.Y. (1997). "Deep-Footing and Wide-Slab effects in reinforced sandy ground." *Journal of Geotechnical and Geoenvironmental Engineering*, ASCE,123(1), pp. 30-36.

14. Huang, C. C., Tatsuoka, F. (1990). "Bearing capacity of reinforced horizontal Sandy ground." *Geotextile and Geomembrane* 9, pp51-82.

15. Ingra, T.S., and Baecher, G.B. (1983). "Uncertainty in bearing capacity of sands." *J. Geotech. Eng.*, ASCE, 109(7), pp. 899-914.

16. Khing, K. H., Das, B. M., Puri, V. K., Cook, E. E., Yen, S. C. (1993). "The bearing capacity of strip foundation on geogrid reinforced sand." *Geotextile and Geomembrane*12, pp351-361.

17. Kolay, P. K., Kumar, S., Tiwari, D. (2013). "Improvement of bearing capacity of shallow foundation on geogrid reinforced silty clay and sand." *Journal of Construction Engineering*.

18. Kumar A., Saran S. (2003). "Bearing Capacity of rectangular footing on reinforced soil." *Geotechnical and Geological Engineering* 21, pp201-224 .

19. Kumar A. ,Ohri M. L., Bansal R. K. (2013). "Pressure Settlement charecteristics of strip footings on reinforced layered soil." *International Journal of Civil and Structural Engineering* Vol. 4, No. 2.



20. Kumar A. ,Ohri M. L., Bansal R. K. (2007). "Bearing capacity tests of strip footing on reinforced layer soil." *Geotechnical and Geological Engineering* 25, pp139-150.
21. Kumar, A., Walia, B. S., Saran, S. (2005). "Pressure-Settlement charecteristics of rectangular footings on reinforced sand." *Geotechnical and Geological Engineering* 23, pp469-481.
22. Latha G.M., Somwanshi A. (2009). "Bearing Capacity of square footings on geosynthetic reinforced sand." *Geotextile and Geomembrane* 27, pp 281-294.
23. Meyerhof G.G. (1953). "An Investigation for the Foundations of a Bridge on Dense Sand." *Proceedings of the 3rd International Conference on Soil Mechanics and Foundation Engineering*, 2, pp. 66-70.
24. Meyerhof G. G. (1963). "Some recent research on the bearing capacity of foundation." *Canadian Geotech. J.* 1(1), pp 16.
25. Michalowski, R. L. (1997). "An estimate of the influence 28. Michalowski, R. L. (1997). "An estimate of the influence of soil weight on bearing capacity using limit analysis." *Soils and Foundations*. 37(4)
26. Milovic, D.M. (1965). "Comparison between the calculated and experimental values of the load carrying capacity." *Proc., 6th ICSMFE, Montreal 1965*, 2, pp. 142-144.
27. Nareeman, B. J. (2012), "A study on the scale effect on bearing capacity and settlement of shallow foundation." *International Journal of Engineering and Technology Volumn 2 No. 3*.
28. Omar, M. T. (2006). "Load carrying capacity of eccentrically loaded strip foundation on geogrid-reinforced sand." *Journal of Pure & Applied Sciences Volumn 3, No. 2*.
29. Patra, C.R., Das, B.M., Atalar, C. (2005). "Bearing capacity of embedded strip

- foundation on geogrid-reinforced sand.” *Geotextiles and Geomembranes*, 23, pp. 454-462.
30. Patra, C.R., Das, B.M., Bhoi, M., Shin, E.C. (2006). “Eccentrically loaded strip foundation on geogrid-reinforced sand.” *Geotextiles and Geomembranes*, 24, pp. 254–259
31. Peck, R. B., Hanson, W. E., Thornburn, T. H., “Foundation Engineering, Second Edition.” *John Wiley & Sons*.
32. Prakash, S., Saran, S. (1971). “Bearing capacity of eccentrically of eccentrically loaded footings.” *Journal of Soil Mechanics and Foundation*, ASCE, 97(1), pp. 95-118.
33. Purkayastha, R.D., Char, R.A.N. (1977). “Sensitivity analysis for eccentrically loaded footings.” *J.Geotech.Eng. Div.*, ASCE, 103(6), 647.
34. Sadoglu E., Cure E., Moroglu B., Uzuner B.A. (2009). “Ultimate load for eccentrically loaded model shallow strip footings on geotextile-reinforced sand .” *Geotextiles and Geomembranes*, 27, pp. 176–182.
35. Sahu, R., Behera, R.N., Patra, C.R., (2013). “Bearing capacity prediction of eccentrically loaded footing on reinforced sand by ANN” *The 5th International Geotechnica Symposium-Incheon, 22-24 May, 2013*, pp.407-414.
36. Shin, E. C., Das, B. M., Lee, E. S., and Ataler, C., (2002). “Bearing capacity of strip foundation on geogrid-reinfoced sand.” *Geotechnical and Geological Engineering* 20: pp169-180.
37. Terzaghi, K., and Peck, R.B. (1948). *Soil mechanics in engineering practice*, 1st Edition, John Wiley & Sons, New York.
38. Vesic, A.S. (1973). “Analysis of ultimate loads of shallow foundations.” *J. of Soil Mech. and Found. Div.*, ASCE, 99(1), pp. 45-73.

